AMMRC 76-30

NOISE ABATEMENT AND INTERNAL VIBRATIONAL ABSORPTION IN POTENTIAL STRUCTURAL MATERIALS

September 1976

L. Kaufman, S. A. Kulin, P. P. Neshe

ManLabs, Inc.
21 Erie Street
Cambridge, Massachusetts 02139

Semi-Final Report Contract Number DAAG46-74-C-0048

Sponsored by: Defense Advanced Research Projects Agency
ARPA Order No. 2555

Program Code No. A13719
Effective Date of Contract: 30 November 1973
Contract Expiration Date: 30 December 1976
Amount of Contract: $635,454.00
Contract Period Covered by Report: 1 September 1975 to 1 March 1976

Approved for public release; distribution unlimited.

Prepared for

ARMY MATERIALS AND MECHANICS RESEARCH CENTER
Watertown, Massachusetts 02172

The view and conclusions contained in this document are those of the authors and should not be interpreted as necessarily representing the official policies, either expressed or implied, of the Advanced Research Projects Agency or the U. S. Government.

The findings in this report are not to be construed as an official Department of the Army position, unless so designated by other authorized documents.

Mention of any trade names or manufacturers in this report shall not be construed as advertising nor as an official indorsement or approval of such products or companies by the United States Government.

DISPOSITION INSTRUCTIONS

Destroy this report when it is no longer needed.
Do not return it to the originator.

UNCLASSIFIED

SECURITY CLASSIFICATION OF THIS PAGE (When Data Entered)

REPORT DOCUMENTATION PAGE		READ INSTRUCTIONS BEFORE COMPLETING FORM
1. REPORT NUMBER AMMRC CTR 76-30	2. GOVT ACCESSION NO. AD-A107	3. RECIPIENT'S CATALOG NUMBER 745
4. TITLE (and Subtitle)		5. TYPE OF REPORT & PERIOD COVERED Semi Final 9/75 to 3/76
		6. PERFORMING ORG. REPORT NUMBER
7. AUTHOR(s)		8. CONTRACT OR GRANT NUMBER(s) DAAG46-74-C-0048
9. PERFORMING ORGANIZATION NAME AND ADDRESS		10. PROGRAM ELEMENT, PROJECT, TASK AREA & WORK UNIT NUMBERS D/A Project: 1T161102AH42 AMCMS Code: 611102.11.H4200 Agency Accession:
11. CONTROLLING OFFICE NAME AND ADDRESS Army Materials and Mechanics Research Center Watertown, Massachusetts 02172		12. REPORT DATE September 1976
		13. NUMBER OF PAGES 80
14. MONITORING AGENCY NAME & ADDRESS(if different from Controlling Office)		15. SECURITY CLASS. (of this report) Unclassified
		15a. DECLASSIFICATION/DOWNGRADING SCHEDULE

16. DISTRIBUTION STATEMENT (of this Report)

Approved for public release; distribution unlimited.

17. DISTRIBUTION STATEMENT (of the abstract entered in Block 20, if different from Report)

18. SUPPLEMENTARY NOTES

19. KEY WORDS (Continue on reverse side if necessary and identify by block number)

Vibration Damping
Ships Propellers
Cobalt-Iron Alloys
Cobalt-Iron Manganese Alloys
Iron-Chromium-Aluminum Alloys
Military Reconnaissence Vehicles

20. ABSTRACT (Continue on reverse side if necessary and identify by block number)

Efforts have been directed toward identifying potential structural materials which can combine high strength and damping characteristics in the audible range. Cobalt-iron alloys with additions of aluminum and manganese, copper-aluminum-nickel alloys, iron-chromium-aluminum alloys, titanium-nickel alloys, and several commercial steel compositions have been investigated. The range of yield strengths and loss factors which are attainable exceed currently available commercial materials.

DD FORM 1 JAN 73 1473 EDITION OF 1 NOV 65 IS OBSOLETE

UNCLASSIFIED

SECURITY CLASSIFICATION OF THIS PAGE (When Data Entered)

A survey of potential applications of high damping alloys to military systems was conducted. Three potential areas which merit consideration include body panels of military reconnaissence vehicles, motor covers and ship propellers. Plans to fabricate body panels for a 1/6 scale dynamic model of an armoured personnel carrier have been made.

Measurements of the enthalpy of transformation in a thermoelastic Cu-Al-Ni alloy has been conducted over a range of grain size and sample size to assess the stored elastic strain energy. Studies of the magnetic domain wall configuration in a cobalt-iron alloy have been initialed to evaluate the contribution of domains to damping in this alloy.

FOREWORD

This research was supported by the Advanced Research Projects Agency of the Department of Defense and was monitored by the Army Materials and Mechanis Research Center under Contract No. DAAG46-74-C-0048.

TABLE OF CONTENTS

LIST OF TABLES

LIST OF FIGURES

LIST OF FIGURES (continued)

LIST OF FIGURES (continued)

1. INTRODUCTION AND SUMMARY

The utilization of structural materials capable of suppressing noise and vibration offers substantial advantages in the design of a wide range of military applications. In particular ship and helicopter propulsion, tracked land vehicle and torpedo propulsion systems would all operate more efficiently if materials capable of absorbing noise and vibration were available for incorporation into the structure.

The present study is aimed at identifying potential structural materials which exhibit high damping capacity (or loss factors) at frequencies in the audible range (i.e. 20-4000 cycles per second) and evaluating the mechanism by which damping takes place. In addition characterization of the mechanical properties such as yield strength and Youngs modulus has also been carried out to evaluate the potential use of the material as a structural element. Finally cost and fabrication factors have also been considered in order to gain some insight into the practical application of these materials in specific military systems.

Novel damping materials such as Nitinol (Ni-Ti) and copper-aluminum-nickel alloys which appear to derive their damping characteristics from thermoelastic martensitic transformations have been investigated. The results have been documented in previous reports (1,2).* In addition, commercial damping materials such as Nivco (Co-Ni-Ti-Al) and Incramute (Cu-Mn-Al) have also been evaluated in order to develop a basis for comparison. In the course of the present study (2) a family of cobalt-iron alloys which can be carefully heat treated to yield very high damping characteristics has been synthesized. Although the mechanism leading to the high loss factors which characterize these alloys is not clear, it appears that the structure which provides the desirable high loss factor is a metastable fcc solid solution. The

*Underscored numbers in parentheses denote references.

80 w/o Co-20 w/o Fe alloy, which is the base for this family, is readily cast, forged and cold worked, has been fabricated into rod by swaging and cold rolled into 50 mil foil so that it could be employed in a variety of applications.

Figure 1 shows a bar graph comparing the loss factors of a number of materials under investigation at present in our study. The 0.2 percent offset yield strength is also shown for each material (please note that the loss factor is shown on logarithmic scale). The commercial materials Nivco and Incramute are in the condition supplied by commercial vendors. The results for Nitinol displayed in Figure 1 have been optimized (2) by applying a 15% reduction in thickness by rolling at room temperature. The bar graphs for Co-Fe, Co-Fe-Al and Co-Fe-Mn represent data taken on annealed samples of the experimental alloys currently under study which have been synthesized in the present program. All of the data displayed in Figure 1 refer to 25°C. The loss factors reported were determined by the resonant dwell method (1,2) using a cantilevered beam at a peak stress of 2000 psi. It is well known that many materials show increased loss factors at higher stress (3-8). Indeed such performance may be of critical importance in actual design. Similarly loss factors (Q^{-1}) are known to vary substantially with frequency and usually increase as the frequency is decreased from the audible range to the 1 cycle/sec range. However present consideration has been restricted to frequencies near 200 Hertz (cycles/sec) at low stress levels.

Figure 1 shows that the Co-Fe alloy can develop loss factors near 0.04 (i.e. 4 percent). However the yield strength is low, 18000 psi. The closest competitor is Incramute which exhibits a loss factor of 2 percent. However Incramute has a higher yield strength, 45000 psi. The remaining commercial material, Nivco, has a low damping capacity near 0.1 percent but a high yield strength of 108,000 psi.

In the past twelve months efforts have been directed

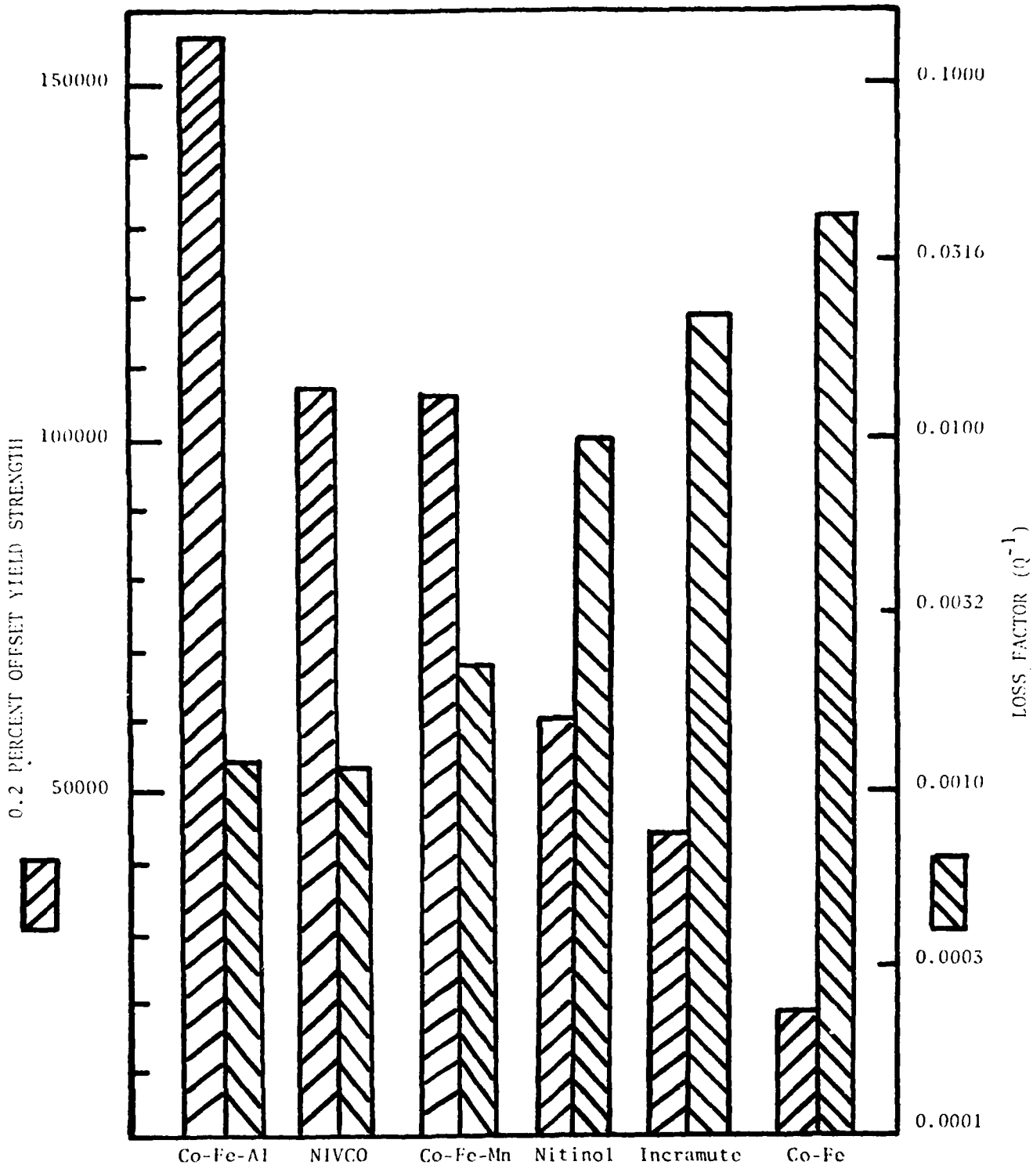

Figure 1. Comparison of Loss Factors and Yield Strength at 25°C for Several Materials. Loss Factor is measured at 2000 psi peak stress and 150-250 Hertz.

towards achieving higher yield strengths in the Co-Fe alloy by additions of nickel, aluminum and manganese. The bar graph in Figure 1 shows results obtained with small additions of aluminum and manganese. In the former case very high yield strengths in excess of 150,000 psi were attained. However this alloy exhibited a loss factor of only 0.1 percent (i.e., like Nivco). Addition of manganese resulted in yield strengths over 100,000 psi coupled with loss factors near 0.3 percent. Thus it appears that a range of loss factors and yield strengths are attainable via alloying the Co-Fe base composition. Current efforts are directed toward optimization of these properties.

An additional facet of the damping factor/mechanical property characteristics of these materials is shown in Figure 2 where the temperature dependence of the loss factor is shown for Nitinol, Incramute and the cobalt-iron alloys. These results indicate that the cobalt-iron alloy maintains high damping characteristics up to 100°C. By contrast Incramute and Nitinol display loss factors below 0.4 percent (i.e, one-tenth that of Co-Fe) above 80°C. Clearly the cobalt-iron alloy offers considerable advantages as a damping material.

During the past six months additional studies of ternary additions to the base 80 w/o cobalt-20 w/o iron composition have been carried out. In particular the effects on aluminum and manganese have been explored. In the case of the former, it was found that very substantial increases in the yield strength (i.e.,from 20,000 psi to 145,000 psi) can be attained on annealed samples of the 80 Co- 20 Fe alloy when the aluminum content increases from 0 w/o to 2.5 w/o. Unfortunately this seven fold increase in strength (which is characterized by a hardness increase from RB 30 to RC 44) is accompanied by a decrease in the loss factor from four percent to 0.2 percent. Although this combination of properties is not attractive for a structural damping material, the hardening effect of aluminum in the cobalt-iron alloys could be employed as the basis for case hardening the

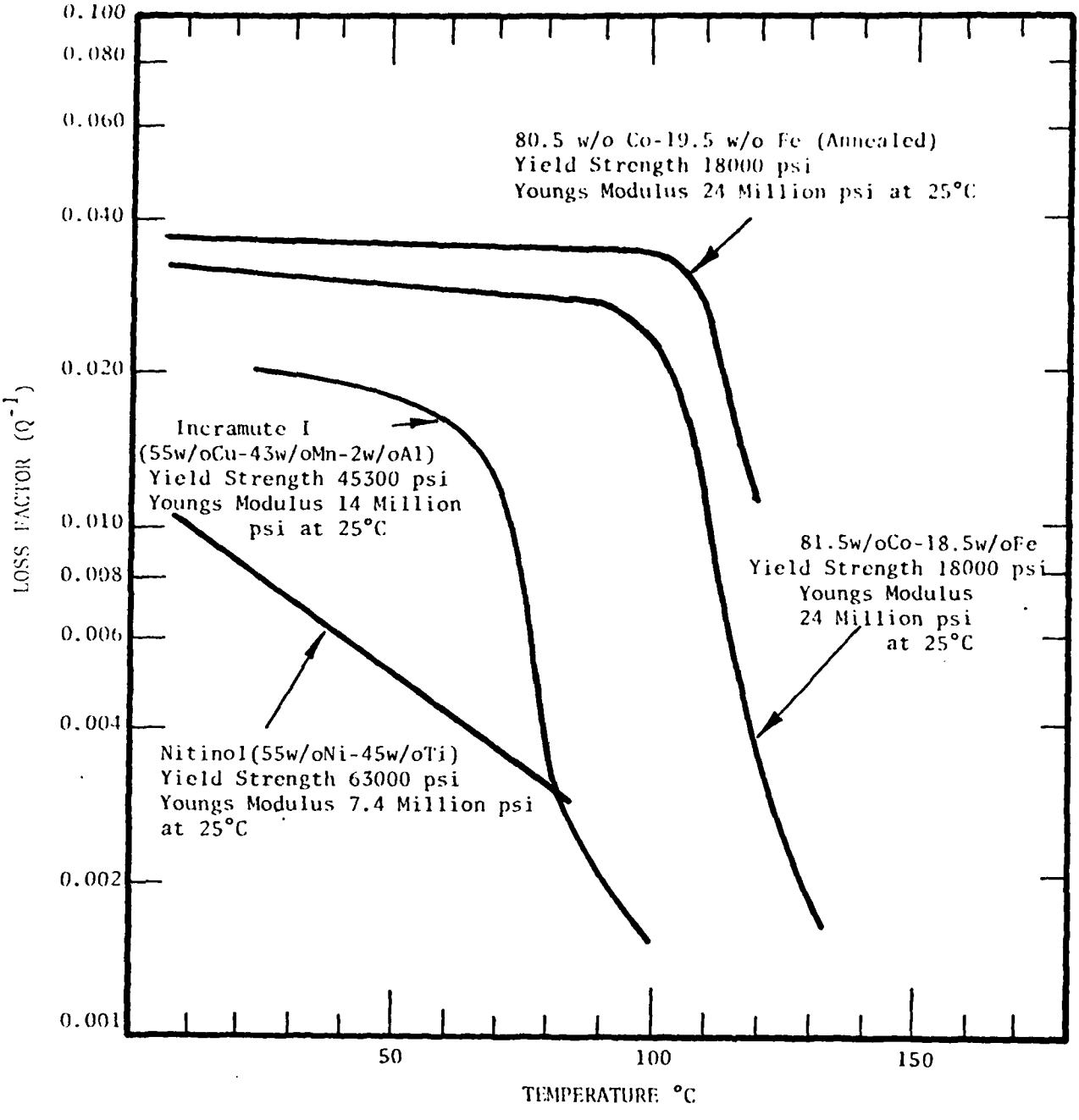

Figure 2. Comparison of the Loss Factor-Temperature Curves for Nitinol, Incramute I and Cobalt-Iron Alloys measured at a stress of 2000 psi in the Frequency Range from 150 to 250 Hertz.

latter where combinations of damping and wear resistance are desired. Manganese additions to the 80 Co-20 Fe base composition were also found to increase the strength and decrease the loss factor. However, current studies of a series of Co-Fe-Mn alloys suggest that a trade-off in properties may be realized with addition of approximately 4 w/o manganese.

Investigation of iron-chromium base alloys (85 w/o Fe-15 w/o Cr-3 w/o Aℓ and 86 w/o Fe-14 w/o Cr-0.05 w/oC) simulating a commercial Japanese damping alloy and type 405 stainless steel has disclosed additional potential damping materials with yield strengths in the 37,000 - 42,000 psi range with good corrosion resistance and yield strengths between 1.5 and 3.5 percent. These materials do not show any decrease in loss factor between - 60°C and 100°C and are relatively inexpensive (i.e., $0.50 to $0.80 per pound). Measurement of the loss factor of the cobalt-iron alloy and the iron-chromium base alloys in a saturating magnetic field lead to a decrease of 15% in the loss factor of the iron-cobalt alloy and a decrease of 30% in the iron-chromium base alloys. Measurement of the loss factor of the 80 w/o Co-20 Fe alloys at 500 psi and 2000 psi yield value of 2% and 4% respectively in keeping with the generally observed relation that the loss factor is proportional to the square root of the stress.

A survey of potential applications of high damping alloys to problems of noise and vibration control was conducted to identify problems areas which could benefit from advances in damping materials technology. Three potential areas appear to merit particular consideration. These include body panels of military reconmissence vehicles, engine oil pans, valve covers, and ship propellers. In each case ancillary properties such as corrosion and/or fatigue resistance must also be maintained in candidate materials if system improvement is to be effected.

One method of evaluating the potential advantages of a candidate high damping structrual material is to fabricate a hull

of this material for the 1/6 scale dynamic model of an armoured personnel carrier constructed by Bolt Beranek and Newman under contract DAAE07-74-C-0002. Plans are being made to carry out such a test on the 80 w/o Co-20 w/o Fe alloy.

Measurements of enthalpy of transformation in a thermoelastic Cu-Al-Ni alloy has been carried out over a range of grain sizes and as a function of sample size in order to assess the stored elastic strain energy contribution on multiple interface transformations. The ability of a thermoelastic martensite to "store" elastic energy is ultimately connected with its capacity to absorb or damp out vibrational energy. If the damping mechanisms is non repeatable then the damping capacity will deteriorate with the amount of energy absorbed. However, if the energy absorbing mechanism is repeatable and the material can return to its original then the damping capacity will not deteriorate. The current measurements of the enthalpy of transformation indicate that the stored elastic strain energy contribution is on the order of 10 cal/mole out of a total enthalpy of transformation of about 120 cal/mole.

Studies of the magnetic domain wall configuration in the 80 Co-20 Fe alloy have been initiated in order to evaluate the contribution of such domains to the damping exhibited by this alloy.

II. INVESTIGATION OF COBALT-IRON ALLOYS FOR APPLICATION AS HIGH DAMPING STRUCTURAL MATERIALS

Current efforts which have been directed toward exploiting the properties of cobalt-iron alloys for the purposes of achieving high damping properties coincident with high strength (2) stem from the work of Cochardt (3,4) who reported on loss factors of 70 w/o Co-30 w/o Ni and Co-Fe alloys at room temperature as disclosed by torsional pendulum measurements at a frequency of one cycle/sec (i.e. one Hertz). Cochardt reported a logarithmic decrement at 25°C and a stress of 2000 psi for a 65 w/o Co-35 w/o Ni alloy of 0.18. The logarithmic decrement is the product of π times Q^{-1}. Thus

$$\zeta = \pi Q^{-1} \tag{1}$$

and if $\zeta=0.18$ then $Q^{-1}\approx 0.06$. This value is approximately fifteen times larger than the value measured in our studies (2). However, the latter values were observed at 200 Hertz (200 cycles/sec) and 2000 psi rather than 1 cycle/sec and 2000 psi stress (2). Cochardt also reported on a 80 w/o Co-20 w/o Fe alloy which exhibited $\zeta=0.09$ (i.e. $Q^{-1}=0.03$) at 1 cycle/sec and 2000 psi and 25°C. This alloy also exhibits a high Curie temperature. However, in the condition as fabricated by Cochardt (3), this alloy was a stable bcc structure which was probably ordered with no chance for transformation. The processing sequence followed by Cochardt called for homogenization at 1100°C for two hours. Figure 3 shows that the alloy was in the fcc field at this temperature (1373°K). Subsequently the alloy was annealed for two hours at 900°C (1173°K). Figure 3 shows that at this temperature the alloy was still in the stable fcc field but just about to enter the two phase fcc+bcc field. The final step in the processing sequence employed by Cochardt was a slow cool to room temperature at the rate of 120°C/hour. During this treatment the sample enters the region where the bcc

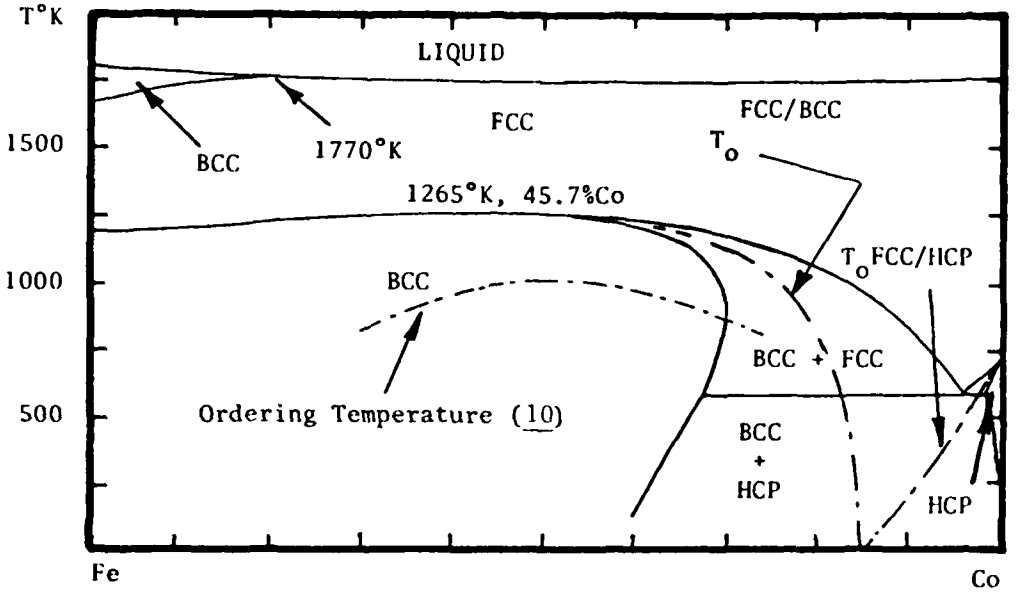

Figure 3. Calculated Iron-Cobalt Phase Diagram Showing Locus of Curve for T_o(FCC/BCC) where FCC and BCC Phases of Same Composition Have Equal Free Energies (9,10).

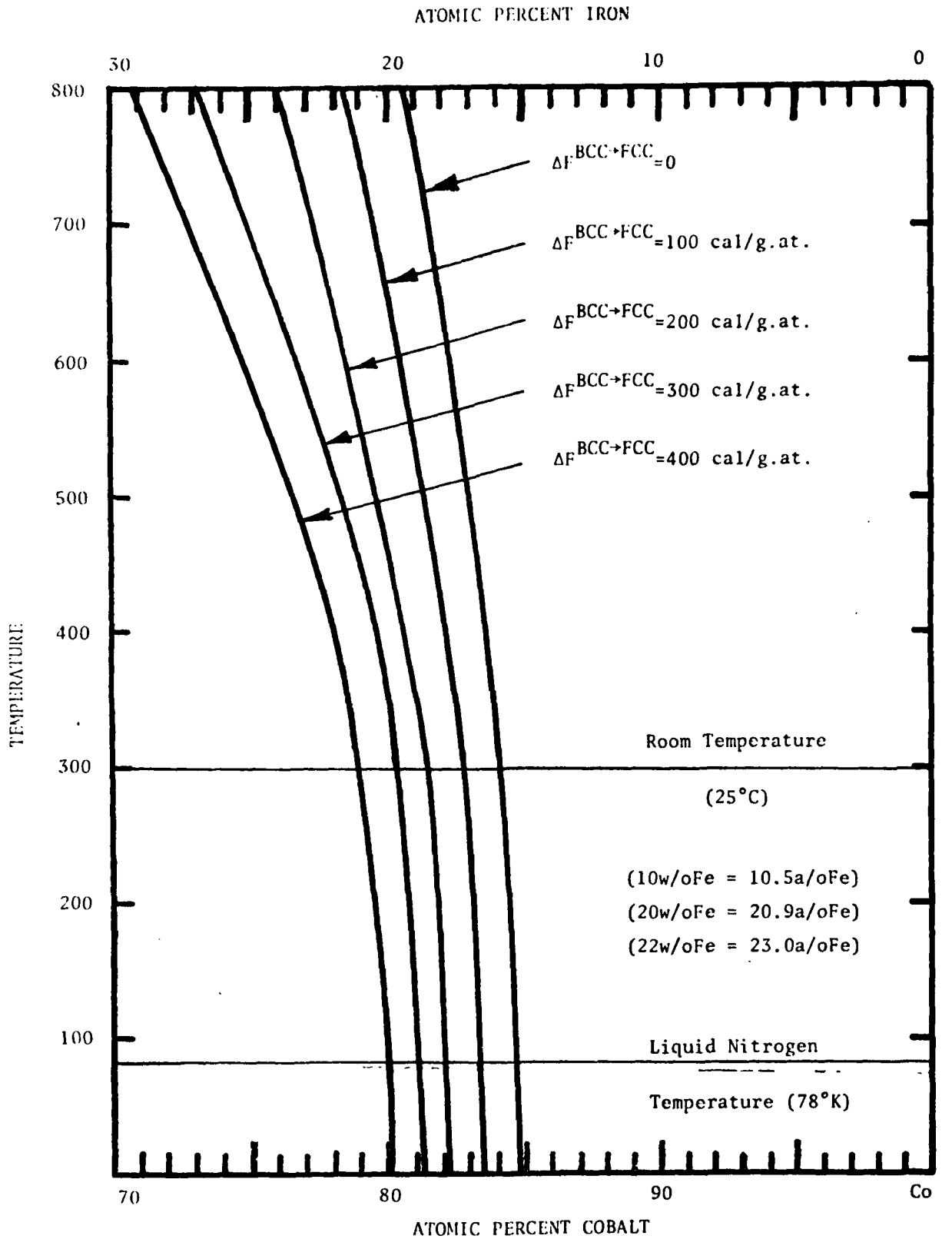

Figure 4. Calculated Temperature and Composition of the Free Energy Difference between FCC and BCC Iron Cobalt Alloys.

phase is stable and coexists with a fcc phase enriched in cobalt. In addition, the bcc orders below 800°K as is seen in Figure 3. Unfortunately Cochardt did not discuss the structure of his 80Co-20Fe alloy. However, based on his heat treatment schedule, it is likely that his alloy was largely bcc.

Figure 3 shows a curve labeled $T_o^{FCC/BCC}$ which describes the locus of points along which the fcc and bcc Co-Fe alloys have equal free energies. This curve has been computed using a thermochemical description of the fcc and bcc phases derived earlier. Figure 4 shows the free energy difference between the fcc and disordered bcc phases as a function of temperature and composition. The curve labeled $\Delta F^{BCC \rightarrow FCC}=0$ is the same as that shown in Figure 3. The remaining curves show the locus of points corresponding to various free energy differences between disordered fcc and bcc phases. As the free energy difference becomes larger, the bcc becomes more stable relative to the fcc phase for a given composition. In the case of iron base alloys (i.e. Fe-Ni and Fe-C alloys), the fcc phase can be retained by rapid cooling until the "driving force" for transformation to the bcc form reaches the vicinity of 300 cal/g.at. (i.e. the free energy of the bcc phase is 300 cal/g.at. less than the fcc phase). Figure 4 suggests that this situation should prevail at room temperature in an alloy with 80 a/o Co-20 a/o Fe (80.9 w/o Co-19.1 w/o Fe). Alloys containing less than 20 a/o Fe could be expected to remain fcc while alloys with greater than 20 a/o (19.1 w/o) Fe would be expected to transform to the bcc phase on cooling from 1000°C. In order to test this prediction, a series of cobalt-iron alloys was prepared and air cooled from 1000°C. Figures 5-8 show the resulting microstructures. The first two photomicrographs show typical austenitic fcc structures obtained by air cooling the 82 w/o Co-18 w/o Fe and 90 w/o Co-10 w/o Fe alloys. On the other hand, Figure 57 shows the martensitic bcc structure obtained on air cooling the 78 w/o Co-22 w/o Fe alloy. The crystal structure

Plate No.
10486

Figure 5. 82 w/o Co-18 w/o Fe Alloy Annealed at 1000°C Air Cooled to 25°C. Etched in 5% Nital. Photomicrograph Shows Twinned Austenitic Structure (X1000).

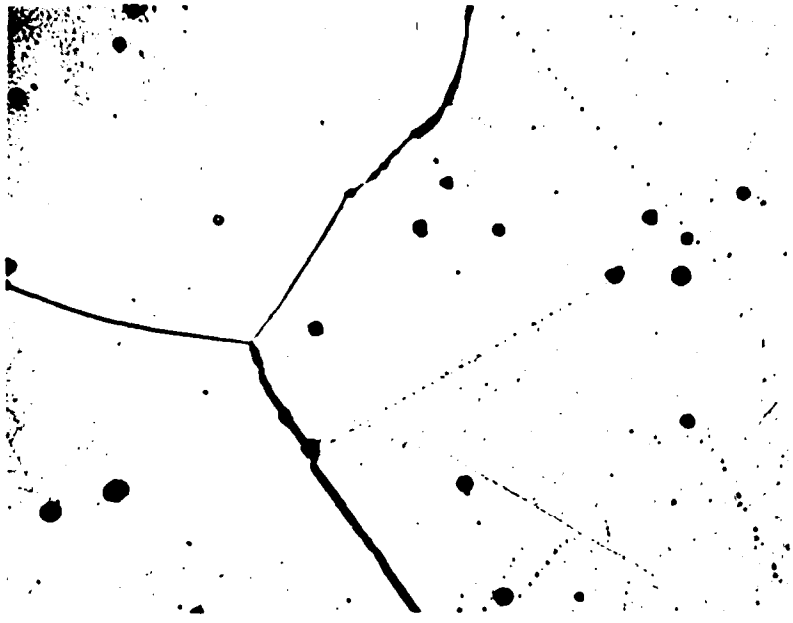

Plate No.
10489

Figure 6. 90 w/o Co-10 w/o Fe Alloy Annealed at 1000°C Air Cooled to 25°C. Etched in 5% Nital. Photomicrograph Shows Twinned Austenitic Structure (X1000).

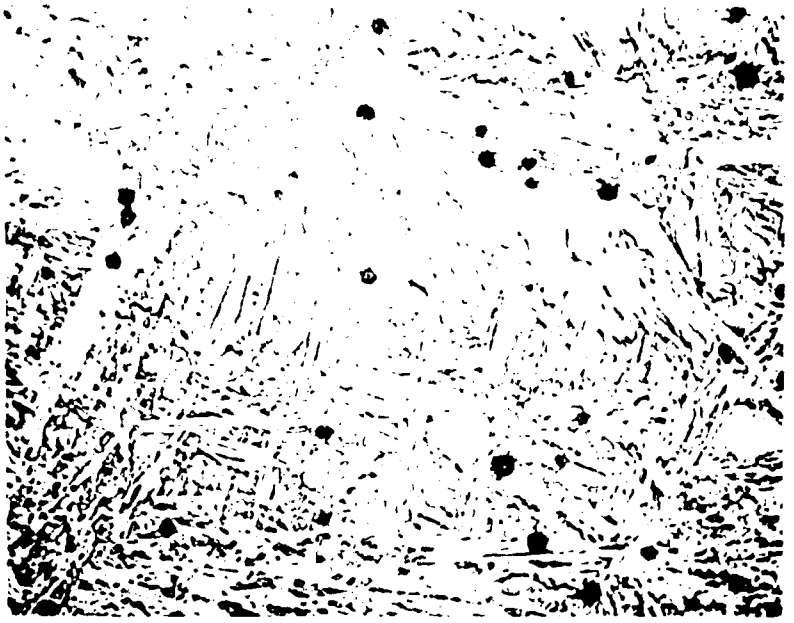

Plate No.
10483

Figure 7. 78 w/o Co-22 w/o Fe Alloy Annealed at 1000°C Air Cooled to 25°C. Etched in 5% Nital. Photomicrograph Shows Structure of BCC Phase (X1000).

Plate No.
10484

Figure 8. 80 w/o Co-20 w/o Fe Alloy Annealed at 1000°C Air Cooled to 25°C. Etched in 5% Nital. Central Grain Shows Surface Martensite (BCC) Formed during Polishing in an Austenite (FCC) Matrix (X1000).

of these alloys was verified by x-ray diffraction using CrKα radiation. Inclusions shown in Figures 5-8 are oxide particles which are present in the Ferrovac E iron used to make the alloy by combination with electrolytic cobalt.

Figure 8 shows the microstructure of the 80 w/o Co-20 w/o Fe alloy which contained some surface martensite formed during the polishing. This was established by annealing the specimen at 1000°C, air cooling it and taking an x-ray pattern from the surface without polishing. This pattern showed no bcc diffraction lines. However, polishing the surface produced strong bcc peaks. This result suggests that the 20 w/o Fe alloy (19.1 a/o Fe) is close to transforming at room temperature. This result is in keeping with the predictions of Figure 4.

An attempt was made to produce martensite in this alloy by cooling it in liquid nitrogen (i.e. to 77°K). However, no bcc phase formed. This may be due to the steep free energy difference versus temperature curve which does not yield very many more cal/g.at. of driving force as the temperature is lowered from 300°K to 77°K.

The results shown in Figures 5-8 are in keeping with earlier studies of the Co-Fe system (11-13) which showed a lowering of the fcc/hcp transition temperature of cobalt by the addition of iron. Addition of 5 a/o Fe to cobalt reduced T_o from 735°K to 500°K (12,13). Alloys with 7.5, 10.0, 12.5 and 15 a/o Fe cooled to 25°C (248°K) by water quenching after two hours at 1100°C were found to be completely fcc (11). Plastic deformation in Liquid nitrogen by hammering to effect a 17% deformation produced hexagonal phase in the 7.5 a/o Fe alloy and some bcc phase in the 15 a/o alloy. However the 10.0 and 12.5 a/o Fe alloys were found to remain fcc.

Thus, the series of Co-Fe alloys shown in Figures 5 and 8 with 18 and 20 w/o iron fall in exactly the range required to test the hypothesis, i.e. that high damping could be attained in

a metastable phase with a high magnetic Curie point. The Curie point for the fcc appears to be near 950°C (1223°K)(13).

Accordingly, a series of "resonant dwell damping" bars were fabricated from alloys in this series and tested at 25°C along with an additional set of alloys at a stress level near 2000 psi. The geometry of the samples resulted in natural frequencies in the 190-270 Hertz range. The results for the original set of samples are shown in Table 1 (2). This group of samples labeled 51-64 were prepared by annealing alloy stock, machining the damping bars and then making the measurements.

Subsequently, the damping bars were x-rayed. It was found that samples 57, 58, 59 and 60 (i.e. 80 w/o Co-20 w/o Fe and 82 w/o Co-18 w/o Fe) exhibited fcc and bcc diffraction lines. This was apparently due to the surface deformation which occurred during machining. Consequently, these four samples were reannealed at 1000°C and oil quenched. These samples yielded completely fcc x-ray patterns. Subsequent measurement of the loss factor yielded values of 280 to 500 x 10^{-4} as shown by samples 57A, 58A, 59A and 60A in Table 1. Following this experience, the remainder of samples 51-64 were reannealed and oil quenched and the loss factor at 25°C measured once again. The results are shown in Table 2. The reannealing did not affect the loss factors of the 78 w/o Co-22 w/o Fe samples very much. These were 14 and 16 x 10^{-4} (Numbers 55 and 56) before the reannealing and 20 and 13 x 10^{-4} (Numbers 55A and 56A) after reannealing. The diffraction patterns both showed substantial quantities of the bcc phase. Similarly, the reannealing had little effect on the 90 w/o Co-10 w/o Fe alloys. The samples 61 and 62 exhibited Q^{-1}=8 and 14 x 10^{-4} before reannealing and 7 and 7 x 10^{-4} after annealing. Both sets of x-ray patterns showed completely fcc structures. Thus the results show a marked peak in the loss factor in the vicinity of 80 w/o Co-20 w/o Fe providing the alloy is all fcc. This is not dependent on the magnetic Curie temperature since both the fcc and bcc phases have high Curie temperatures which

TABLE 1

SUMMARY OF RESONANT DWELL DAMPING MEASUREMENTS AT 25°C

Sample No. Composition (weight percent)	Resonant Frequency (Hz.)	Dynamical Youngs Modulus ($PSIx10^{-6}$)	Peak Stress (PSI)	Loss Factor ($Q^{-1}x10^{4}$)	Comments on Test
51(70Co-30Ni)	265	28.0	2190	66	All Samples
52(47.2Fe-52.8Pt)	185	15.7	1290	28	Annealed at
53(47.2Fe-52.8Pt)	214	19.2	1660	25	1000°C--Air
54(46.2Fe-53.8Pt)	191	14.7	1290	69	Cooled--Then
55(78.0Co-22.0Fe)	259	26.6	2050	14	Machined
56(78.0Co-22.0Fe)	251	26.3	1980	16	"
57(80.0Co-20.0Fe)	237	24.2	1790	92	"
58(80.0Co-20.0Fe)	251	24.3	1900	68	"
59(82.0Co-18.0Fe)	245	23.1	1800	81	"
60(82.0Co-18.0Fe)	237	22.8	1740	64	"
61(90.0Co-10.0Fe)	264	27.8	2140	8	"
62(90.0Co-10.0Fe)	264	28.1	2140	14	"
63(65Co-28Fe-7Ni)	240	23.2	1770	17	"
64(70Fe-20Co-10Cr)	276	29.9	2410	6	"
57A(80.0Co-20.0Fe)	238	24.4	1810	280	All Samples
58A(80.0Co-20.0Fe)	243	25.5	1990	450	Annealed at
59A(82.0Co-18.0Fe)	236	21.4	1670	480	1000°C and
60A(82.0Co-18.0Fe)	242	23.8	1810	500	Oil Quenched

TABLE 2

SUMMARY OF RESONANT DWELL DAMPING MEASUREMENTS AT 25°C

Sample No. Composition (weight percent)	Resonant Frequency (Hz.)	Dynamical Youngs Modulus ($PSI \times 10^{-6}$)	Peak Stress (PSI)	Loss Factor ($Q^{-1} \times 10^{4}$)	Comments on Test
55A(78.0Co-22.0Fe)	253	25.4	1960	20	All Samples
56A(78.0Co-22.0Fe)	252	26.5	2000	13	Annealed at
61A(90.0Co-10.0Fe)	266	28.2	2170	7	1000°C--Then
62A(90.0Co-10.0Fe)	272	29.8	2270	7	Oil Quenched
63A(65Co-28Fe-7Ni)	244	24.0	1830	28	"
72A(79.0Co-21.0Fe)	249	24.3	1900	19	"
73A(79.0Co-21.0Fe)	264	27.8	2140	10	"
75A(80.0Co-20.0Fe)	249	24.3	1900	24	"
76A(80.0Co-20.0Fe)	251	26.3	1980	274	"
77C(81.0Co-19.0Fe)	232	21.2	2000	11	Machined in 33%
78C(80.5Co-19.5Fe)	248	24.3	2000	12	Cold Worked Condition
79 NIVCO	275	28.3	2000	14	As Received from
79 NIVCO	272	28.2	5000	26	Westinghouse
80C(81.5Co-18.5Fe)	245	23.1	2000	12	Machined--Cold Worked
73B(79.0Co-21.0Fe)	263	27.0	2100	9	Annealed--Water Quenched
77A(81.0Co-19.0Fe)	257	24.8	2000	31	Annealed 1000°C--Then
78A(80.5Co-19.5Fe)	248	24.4	2000	320	Oil Quenched
80A(81.5Co-18.5Fe)	247	24.3	2000	110	"

are near 1000°C.

Table 2 shows additional results for other Co-Fe alloys with compositions in the vicinity of 80 w/o Co-20 w/o Fe which were made and tested in order to establish the effects of composition, structure and degree of cold work on the loss factor. These preliminary results show that the high damping behavior can be reproduced in other alloys but it is eliminated by cold work. This work is proceeding in order to establish the processing limits for obtaining high loss factors.

Table 2 also contains the results of damping tests on NIVCO, which is a commercial alloy developed by Cochardt at Westinghouse (4). It was kindly furnished by Dr. Lou Willertz of Westinghouse Research Laboratories. According to Cochardt's description, NIVCO is 72 w/o Co-23 w/o Ni and the balance titanium and aluminum which are added to provide strength by precipitation hardening. Cochardt reports values of the logarithmic decrement of 0.02 and 0.05 at room temperature for this alloy at shear stresses of 2000 psi and 5000 psi (Figure 1 of Reference 4). Since Q^{-1} is equal to the decrement divided by π, Cochardt's results would correspond to loss factors of 0.007 and 0.017 or 70×10^{-4} and 170×10^{-4} respectively at 25°C and stresses of 2000 psi and 5000 psi. These values are much higher than those shown in Table 2. The values measured in the present tests, i.e. 14×10^{-4} at 2000 psi and 26×10^{-4} at 5000 psi, are five times smaller than Cochardt's results. The main difference is that the frequency of the present measurements at 230-270 Hz is in the audible range while that used by Cochardt was near 1 cycle/sec (1 Hertz).

The results (2) shown in Tables 1 and indicate that loss factors of $Q^{-1} = 500 \times 10^{-4}$ are attainable in the 80 w/o Co-20 w/o Fe alloys which are two to three times higher than observed in Nitinol (i.e. 55 w/o Ni-45 w/o Ti) and fifty times higher than NIVCO. Preliminary results on the 80 w/o Co-20 w/o Fe alloy show almost no change in the audible "ring" (or lack of

"ring") of the alloy at liquid nitrogen or +200°C. Thus it is not anticipated that the Q^{-1} value will decrease significantly in this temperature range.

The other advantages the Co-Fe alloy has in relation to the Ni-Ti alloy are a higher modulus of 25 million psi (Tables 1 and 2) versus 8 million psi and the ease with which the Co-Fe alloy can be fabricated.

In order to evaluate the strength of the 80 w/o Co-20 w/o Fe composition, a set of tensile bars were fabricated of annealed material. Subsequent tests were expanded to test swaged rod. These were compared with tensile results measured for NIVCO (2). The 82 w/o Co-18 w/o Fe and 80 w/o Co-20 w/o Fe alloys show reproducible 0.2 percent offset yield strengths of 17000-18000 psi in the annealed condition. This is the strength level of the samples which exhibited loss factors of $Q^{-1} = 500 \times 10^{-4}$. The yield strength was also measured for samples of the 18.5 w/o Fe, 19 w/o Fe and 19.5 w/o Fe alloys in a cold worked condition following a 33% reduction in diameter by cold swaging. In this condition yield strengths near 70,000 psi were observed (2). Reference to Table 2 shows that these alloys exhibited loss factors of 11 to 14 $\times 10^{-4}$ in the cold worked condition. Annealing raised the loss factor of the 19.5 w/o Fe sample to 320 $\times 10^{-4}$ as shown in Table 2.

Tensile tests on NIVCO produced a 0.2 percent yield strength of 108,900 psi (2) in good agreement with Cochardt's reported value of 110,000 psi (4).

These values of the yield strength were combined with the measured loss factors measured at a stress level of 2000 psi in the range 150 to 250 Hz for NIVCO, 80 w/o Co-20 w/o Fe and 55 w/o Ni-45 w/o Ti are compared in Figure 1. The comparison shows the relatively high damping capacity (and low strength) of the Co-Fe alloy to the other two materials. However, it is likely that this shortcoming can be overcome through alloying. For example, the strength of NIVCO is not due to the properties

of the 72 w/o Co-23 w/o Ni matrix, which is comparable to the 80 w/o Co-20 w/o Fe material. The strength is due to the presence of precipitates formed by the Al and Ti additions. A similar effect can be expected in the Co-Fe alloy. Another possible source of strengthening is additional solid solution hardening which might be effected by addition of nickel. The nickel additions would be controlled so as to maintain the "metastable condition" of the fcc phase. This is illustrated in Figure 9 which shows the ternary Fe-Ni-Co counterpart of Figure 3 calculated on the basis of the thermochemical description published previously (9).

Figure 9 shows the locus of the $\Delta F^{BCC \rightarrow FCC}=0$ and the $\Delta F^{BCC \rightarrow FCC}=+300$ cal/g.at. curves in the Fe-Ni-Co system at 25°C. These alloys should be metastable in the fcc form at 25°C. If they can be fabricated in this state, they may develop high Q^{-1} values comparable to 80 w/o Co-20 w/o Fe and higher yield strengths than the 17,500 psi level exhibited by the 80/20 Co-Fe alloy. Such a series of alloys is currently being fabricated for evaluation. If this effort produces the desired result, it would also have a beneficial effect on the cost of the alloys since it would increase the iron content of the alloy and substitute nickel for cobalt. Both of these composition changes would lower the cost.

In order to proceed with the development of the 80 w/o Co-20 w/o Fe compositions, two separate routes have been pursued. First, fabrication studies on the base composition have been pursued. Second, alloying studies have been carried out in order to evaluate the effects of additions on the strength and damping capacity. All of the measurement techniques employed in these tests are those which have been detailed in earlier reports (1,2).

Three ten-pound heats of the 80 w/o Co-20 w/o Fe alloy have been vacuum melted and cast into two inch diameter moulds. The ingots were subsequently forged to 3/4 inch bars and then (cold) swaged to 1/2 inch rod. Intermediate anneals of 1000°C

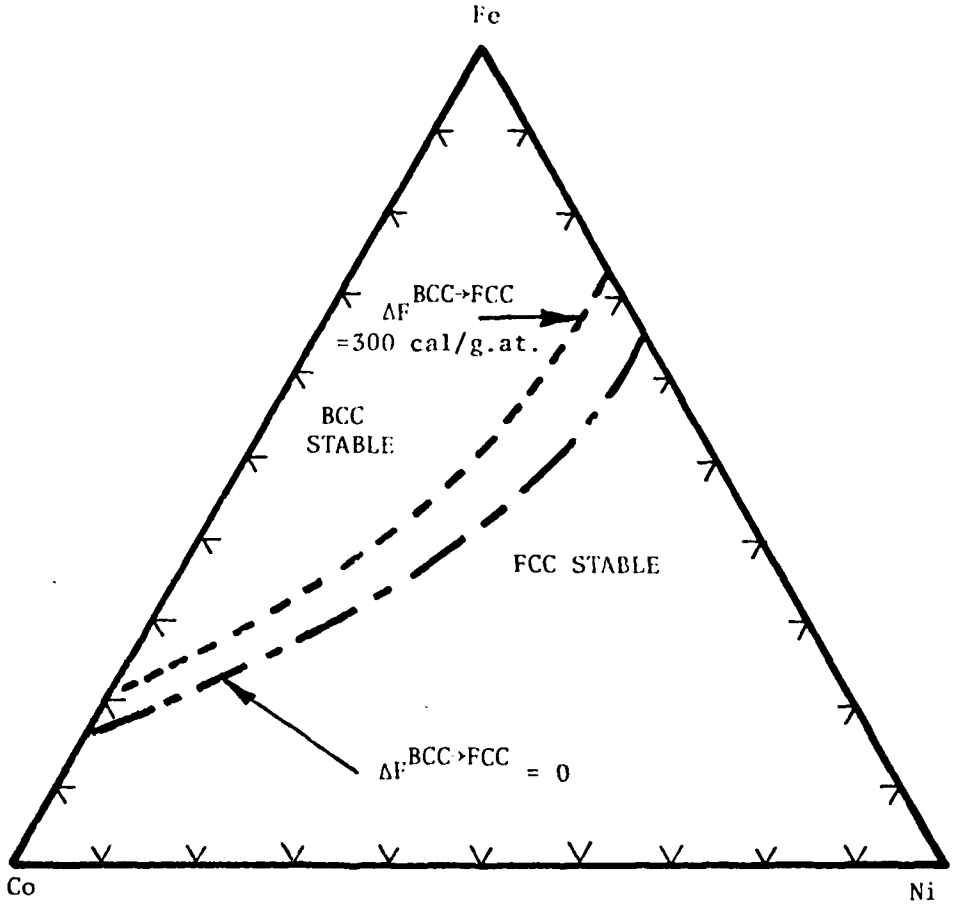

Figure 9 . Calculated Regions of BCC and FCC Stability for Fixed Compositions at 25°C in the Iron-Nickel-Cobalt System.

were employed. The final product was sixty inch long rod. However, it was found that this structure was a mixture of bcc and fcc phases (see earlier discussion) and the rod "rang" when struck, indicating poor damping. However, the high damping characteristics were readily restored by proper heat treatment above 1000°C followed by air cooling. The x-ray analysis of the material disclosed a fully austenitic (fcc) structure and the high damping characteristic of the rod was regenerated.

A second demonstration of the ease with which the 80 w/o Co-20 w/o Fe alloy can be fabricated was the reduction of as-cast 1/2 inch thick slab to 50 mil foil. This was carried out in a series of 20% reductions with intermediate anneals. The reductions were quite moderate and the ease with which they were made indicates that even larger reductions could be successfully carried out. This would certainly appear to be possible if the reductions were carried out by hot rolling. The final treatment of the fifty mil foil consisted of a 1000°C for 30 minutes which yielded soft foil which "rang like lead."

These results indicate that the 80 w/o Co-20 w/o Fe alloy can be readily formed if it is in the fcc condition. Moreover it can be heat treated to yield this structure quite readily. Although it has been established that the two phase (fcc+bcc) structure does not exhibit outstanding damping characteristics, it is probable that rather high strengths could be attained with this structure if it were attained by formation of an ordered bcc phase. This alloy (80 w/o Co-20 w/o Fe) could be readily formed in the fcc structure (as demonstrated above) and then aged to high strength by ordering the bcc phase. In fact, small carbon additions might even be incorporated into such a structure to enhance the strength by conferring some tetragonality into the bcc phase in analogy with ferrous martensites.

Before turning to the alloying studies conducted on the 80 w/o Co-20 w/o Fe alloy it is useful to recount the temperature dependent studies undertaken to establish the data shown in Figure

2. The tests were conducted under the direction of Dr. John Heine of Bolt Beranek and Newman using the techniques detailed earlier (1,2).

Figures 10 and 11 show loss factor versus temperature curves for samples of a 80.5 w/o Co-19.5 w/o Fe and 81.5 w/o Co-18.5 w/o Fe alloy between -60°C and +80°C. Additional samples which were tested between 25°C and 130°C yield the results shown in Figure 2.

In order to obtain an additional set of data on a high damping alloy which is generally available, a sample of Incramute was obtained from Mr. Eugene Thiele of the Copper Development Association Inc. A square plate 5 1/2 inches x 5 1/2 inches x 1/4 inch thick was obtained in the heat treated condition designed to yield maximum damping. This plate was employed to fabricate resonance dwell damping bars (1,2) and tensile bars. Figure 12 shows the results of the damping measurements conducted on the Incramute (55 w/o Co-43 w/o Mn-2 w/o Al) alloy between -60°C and 100°C. Tensile tests conducted at 25°C resulted in a 0.2% offset yield strength of 45,300 psi. These data are shown in Figures 1 and 2.

It is interesting to note that the copper-manganese alloy system, upon which Incramute and several other commercial damping alloys are based was predicted to have a metastable fcc miscibility gap in 1969 (14). Recent experimental studies by Vitek and Warlimont and by Ye. Z. Vintaykin and coworkers (16) have verified this prediction and Figure 13 shows that the metastable miscibility gap in the fcc phase of this system provides the basis for attaining high damping in Incramute and other Cu-Mn alloys via heat treatment.

The second phase of the study of damping in the 80 w/o Co-20 w/o Fe alloy currently under investigation is the evaluation of alloying additions on damping and strength. These activities were initiated during the past three months and have thus far demonstrated that substantial increases in strength can be obtained. However, the optimum "trade off composition" has not yet

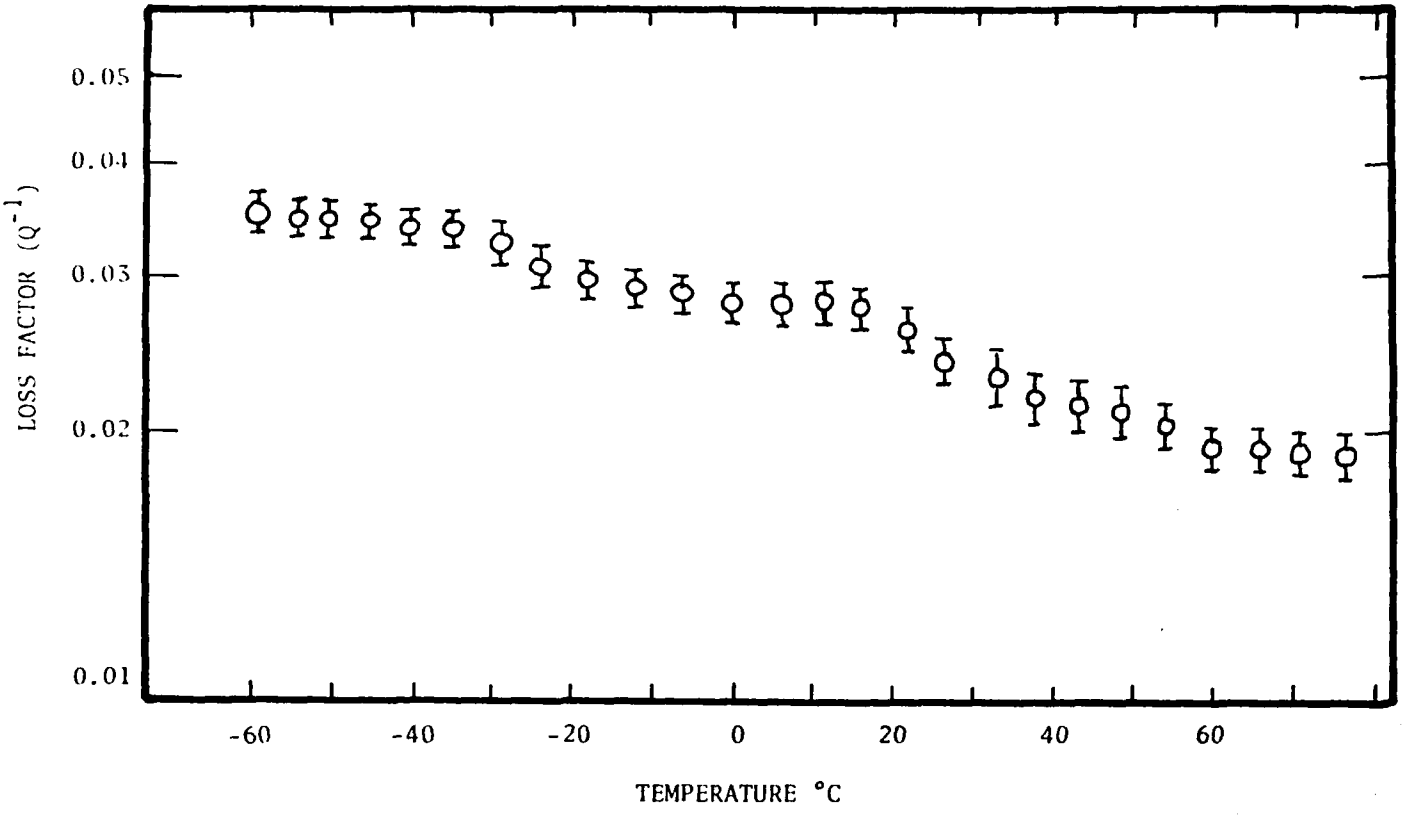

Figure 10. Loss Factor vs. Temperature Curve for a Sample of 80.5 w/o Co-19.5 w/o Fe measured at 240-250 Hertz and a stress of 2000 psi. The dynamical Young's Modulus measured over the same temperature range varied from 24 million psi at -60°C to 23 million psi at +80°C. The sample was annealed at 1000°C and air cooled.

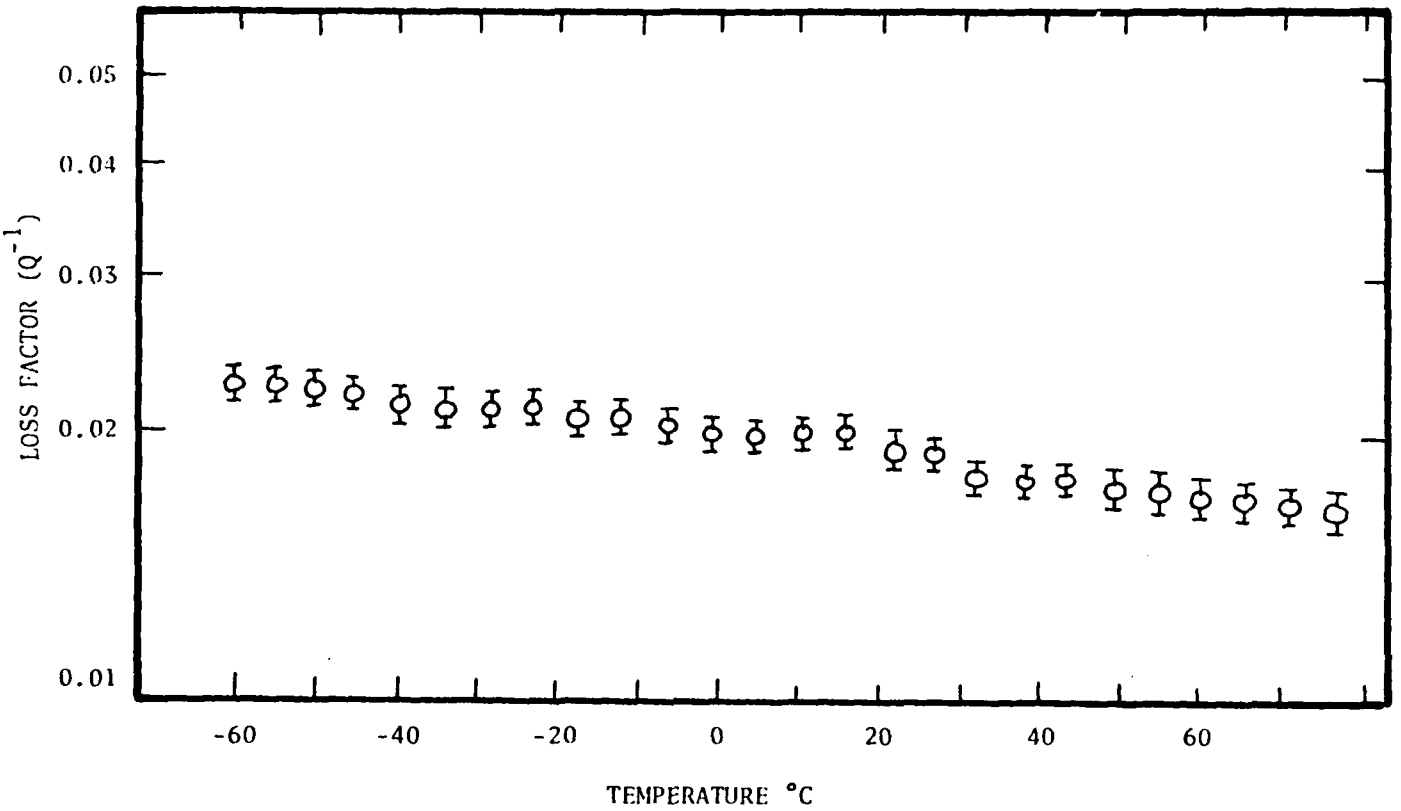

Figure 11. Loss Factor vs. Temperature Curve for a Sample of 81.5 w/o Co-18.5 w/o Fe measured at 240-250 Hertz and a stress of 2000 psi. The dynamical Young's Modulus measured over the same temperature range varied from 24 million psi at -60°C to 23 million psi at +80°C. The sample was annealed at 1000°C and air cooled.

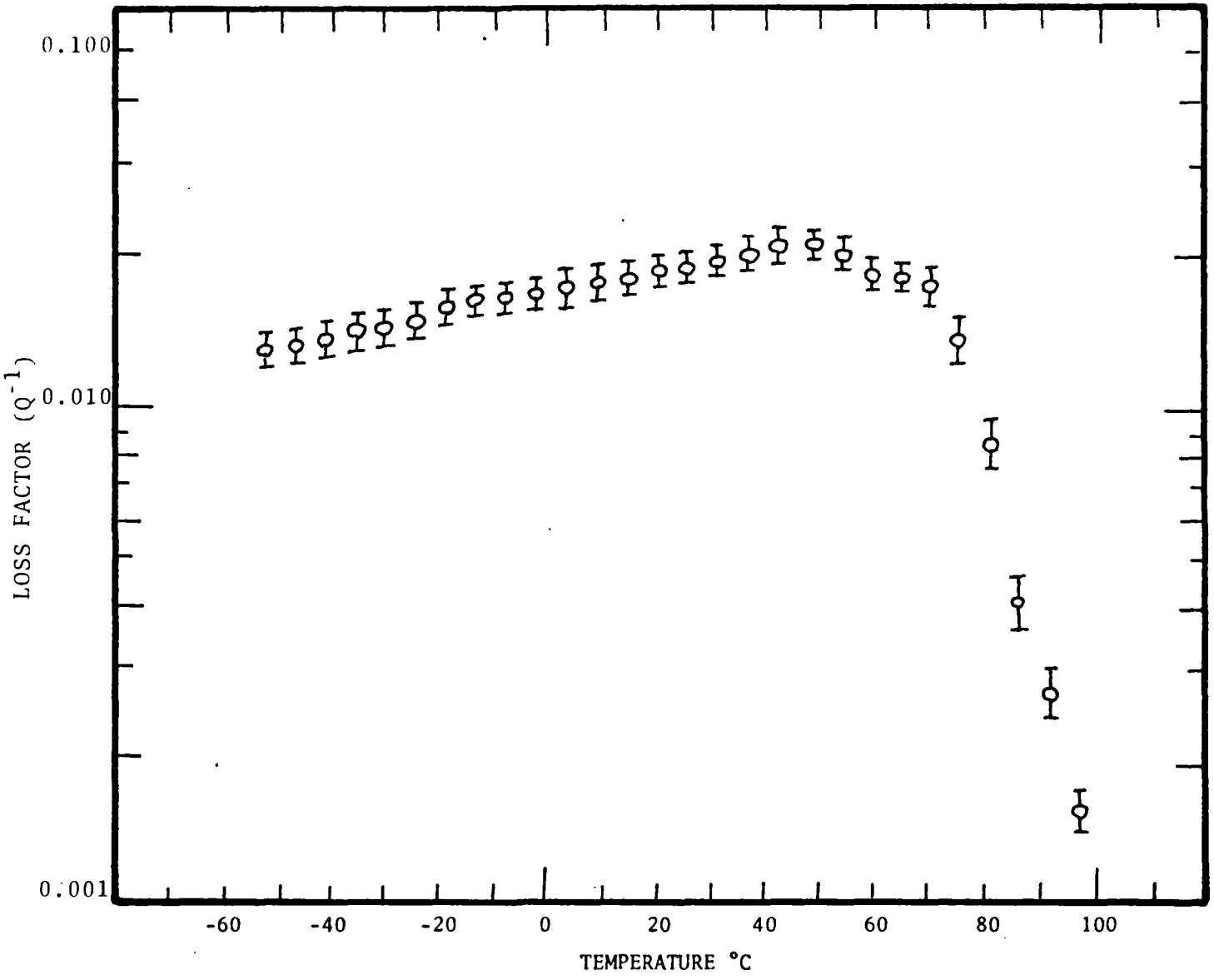

Figure 12. Loss Factor vs. Temperature for a Sample of Incramute I (Nominal Composition 55 w/o Cu-43 w/o Mn-2 w/o Al) heat treated for maximum damping characteristics and measured at 180-220 Hertz at a peak stress of 2000 psi. The dynamical Youngs Modulus varied from 12.5 Million psi at 100°C to 15.5 Million at -60°C.

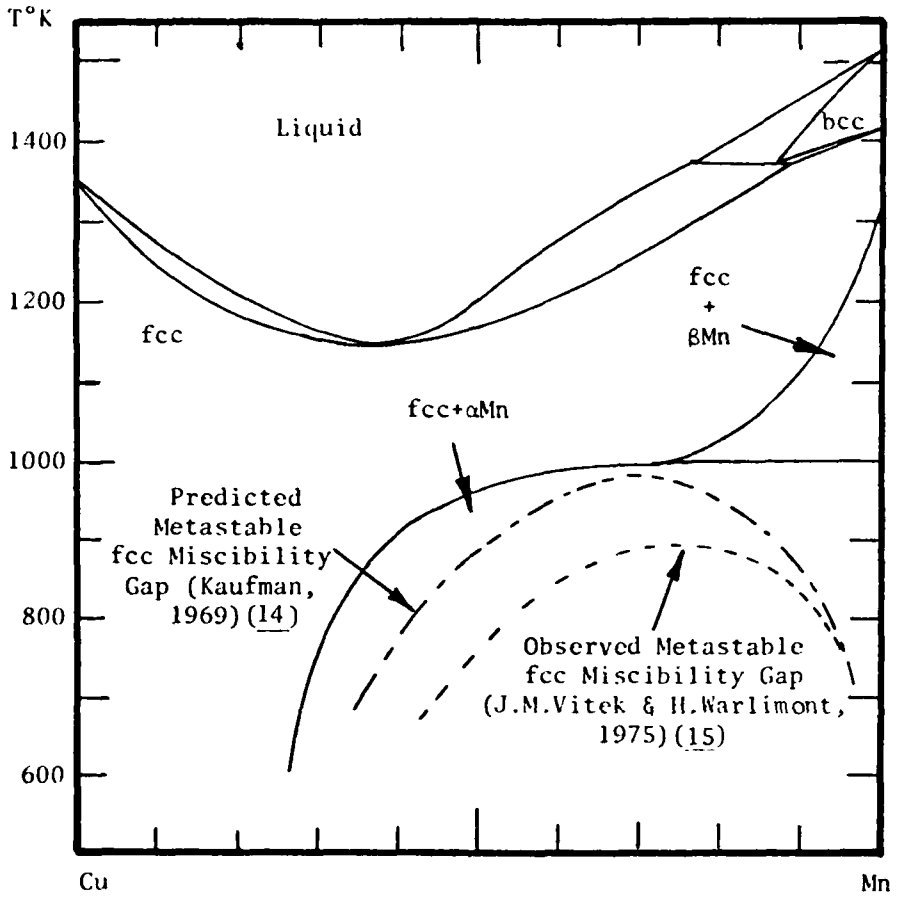

Figure 13. Predicted (14) and Observed (15) Metastable Miscibility Gaps in the Cu-Mn System.

been identified.

Table 3 shows the preliminary results which have been obtained. This compilation shows results of alloys synthesis, fabrication damping and tensile tests on eight alloys based on the Co-Fe composition with substanital additions of nickel or small additions of manganese or aluminum. These results were employed in construction the bar graph shown in Figure 1.

The results obtained thus far indicate that the additions of nickel do not offer any substantial improvement in strength. However, very substantial increases in strength have been attained with aluminum and manganese. These improvements have been accompanied by a decrease in damping capacity. Nevertheless it is interesting to note that sample number 102 (76 w/o Co-19 w/o Fe-5 w/o Mn) exhibited twice the damping capacity of NIVCO at a comparable strength level (see Figure 1) while sample 99 (76 w/o Co-18 w/o Fe-5 w/o Al) exhibited a yield strength of 182,000 psi versus 110,000 psi for NIVCO at the same level of damping capacity which NIVCO exhibits (2).

Table 4 summarizes the results of damping and mechanical property measurements conducted on a series of cobalt-iron and cobalt-iron base alloys to which additions of manganese, chromium and aluminum have been made. In each case evaluation of the damping and yield strength have been made on samples which were cold worked by rolling (to 10% reduction in thickness) as well as on companion samples annealed at 1000°C and air cooled.

The results obtained with sample composition 111 and 112 indicate a very abrupt change in behavior when the aluminum content is increased from 2.5 w/o (i.e., samples 97 and 98 in Table 3) to 3 w/o (i.e., samples 111 and 112 in Table 4). As was noted previously (2) aluminum additions result in subtantial increases in the tensile strength of the cobalt-iron which are accompanied by similar decreases in the loss factor. The compositions corresponding to 111 and 112 represented an attempt

TABLE 3

SUMMARY OF 0.2 PERCENT OFFSET YIELD STRENGTH AND
RESONANT DWELL DAMPING MEASUREMENTS AT 25° (Peak Stress 2000 PSI)
(ALL SAMPLES WERE MACHINED THEN ANNEALED
AT 1000°C AND AIR COOLED)

Sample No. Composition (weight percent)	Resonant Frequency (Hz.)	Dynamical Youngs Modulus (PSI x 10^{-6})	Loss Factor	0.2 Percent Offset Yield Strength (PSI)
85-(60Co-28Fe-12Ni)	243	24.0	0.0026	23100
86-(60Co-28Fe-12Ni)	246	24.6	0.0056	32400*
87-(50Co-32Fe-18Ni)	243	24.0	0.0026	30000
88-(40Co-38Fe-22Ni)	225	20.6	0.0016	29800
94-(72Co-18Fe-10Mn)	264	28.3	0.0011	53700
95-(72Co-18Fe-10Mn)	275	30.7	0.0008	87700*
97-(78.5Co-19Fe-2.5Aℓ)	255	26.4	0.0015	25000
98-(78.5Co-19Fe-2.5Aℓ)	240	23.4	0.0029	29900*
99-(76Co-18Fe-6Al)	273	30.3	0.0013	182000
100-(76Co-18Fe-6Al)	268	29.2	0.0011	157000*
101-(76Co-19Fe-5Mn)	262	27.9	0.0010	83800
102-(76Co-19Fe-5Mn)	264	28.3	0.0027	105700*
103-(77Co-19Fe-4Al)	271	30.1	0.0015	145000
104-(77Co-19Fe-4Al)	269	29.4	0.0011	152000*

*Cold Worked

TABLE 4

SUMMARY OF 0.2 PERCENT OFFSET YIELD STRENGTH AND RESONANT DWELL DAMPING MEASUREMENTS AT 25°C (Peak Stress 2000 PSI) (SAMPLES WERE MACHINED IN THE COLD WORKED CONDITION AND TESTED DIRECTLY OR ANNEALED AT 800°C or 1000°C (AN800, AN1000) AND AIR COOLED BEFORE TESTING)

Sample No. Composition (weight percent)	Condition	Resonant Frequency (Hz.)	Dynamical Young's Modulus (PSI x 10^{-6})	Loss Factor	0.2 Percent Offset Yield Strength (PSI)
106A-(78Co-20Fe-2Mn)	AN1000	248	24.2	0.0400	18000
106B-(78Co-20Fe-2Mn)	CW	250	24.3	0.0020	45000
107 -(72Co-18Fe-10Cr)	AN1000	238	23.8	0.0078	20000
108 -(72Co-18Fe-10Cr)	CW	237	23.8	0.0040	26000
109 -(80Co-20Fe)	AN1000	243	24.0	0.0400	17400
110 -(80Co-20Fe)	CW	249	24.3	0.0090	25000
111 -(77Co-19Fe-3Aℓ)	AN1000	267	27.9	0.0009	78000
112 -(77Co-19Fe-3Aℓ)	CW	270	28.5	0.0008	113000
113 -(77.2Co-19.2Fe-3.6Mn)	AN1000	247	24.2	0.0270	18000
114 -(77.2Co-19.2Fe-3.6Mn)	CW	247	24.2	0.0042	24800
115 -(76.4Co-19.2Fe-4.4Mn)	AN1000	254	26.2	0.0009	67000
116 -(76.4Co-19.2Fe-4.4Mn)	CW	255	26.3	0.0008	106000

to effect an increase in strength without experiencing a decrease in damping by operating at a composition close to that of samples 97 and 98. Unfortunately however, the desired increase in strength (to 78,000 psi) in the annealed condition was accompanied by a drop in damping.

Although the studies of aluminum additions have been disappointing in the sense that an alloy combining high damping and high strength has not been identified, the observation that small additions of aluminum result in substantial strength and corresponding increases in hardness (RB 30 for 0 w/o Al to RC 44 for 4 w/o Al) in the annealed condition may be of practical value. In particular, in the event an application demanding high damping and high hardness should present itself, it might be possible to "alluminize" an 80 Co- 20 Fe alloy and obtain a wear resistant surface on a component with a high loss factor.

The results obtained with additions of chromium to the base cobalt-iron composition as disclosed by sample composition 107 and 108 suggest modest increases in strength accompanied by subtantial decreases in loss factor. Accordingly further studies of chromium additions have been curtailed.

As indicated in the previous report (2), additions of manganese were observed to provide an avenue for increasing the strength of the cobalt-iron alloys. Table 4 summarizes the results obtained on an additional series of cobalt-manganese alloys investigated during the present period. These results, which are shown graphically in Figure 14 suggest that a "trade-off" between strength and damping can be optimized at about 4 w/o Mn. An alloy of this composition is currently being fabricated.

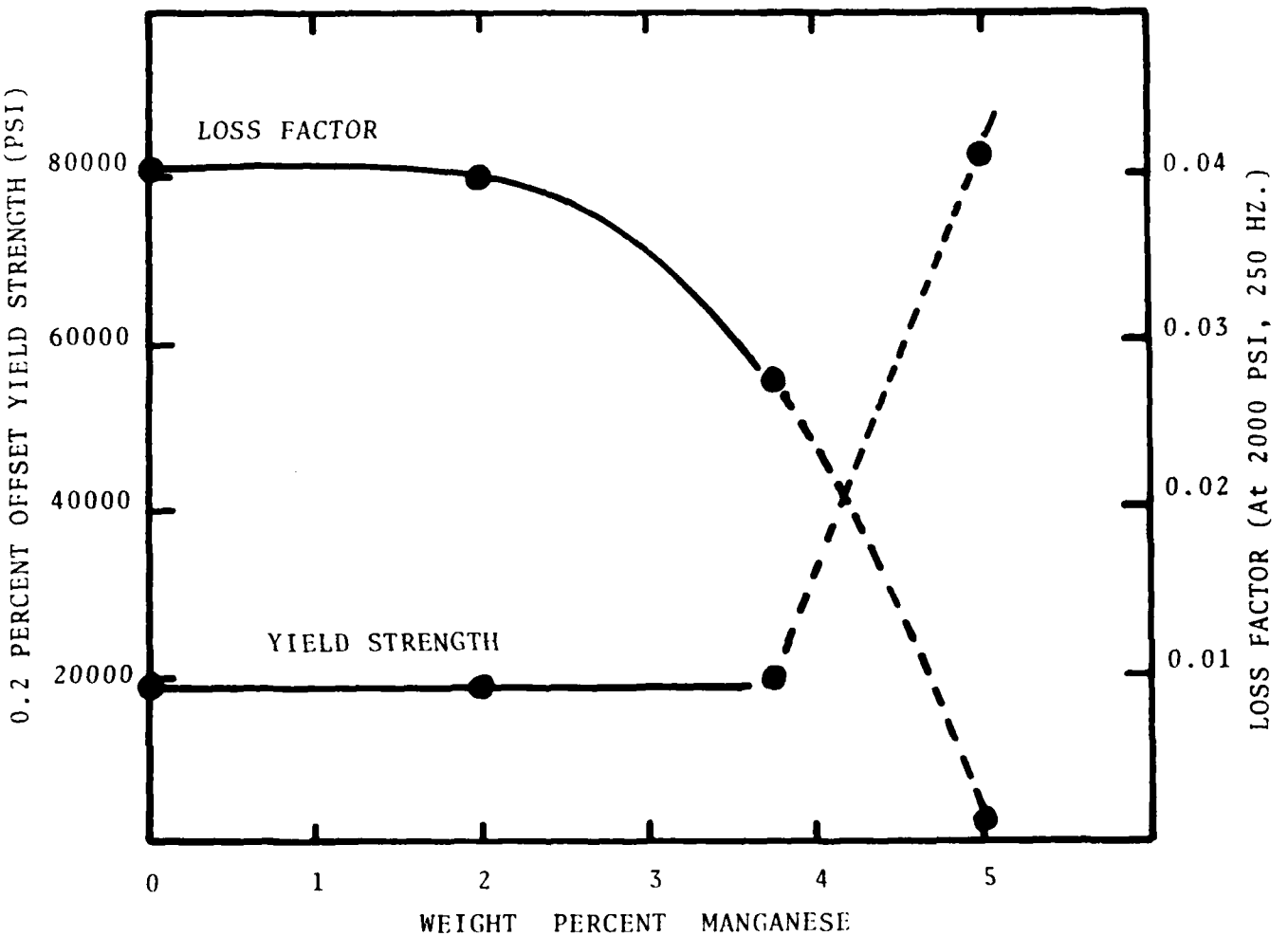

Figure 1 . Loss Factor and 0.2 Percent Offset Yield Strength vs Manganese Content for a series of Cobalt-Iron-Manganese Alloys.

III. INVESTIGATION OF IRON - CHROMIUM ALLOYS FOR APPLICATION AS HIGH DAMPING STRUCTURAL MATERIALS

One of the main short comings of the cobalt - base alloys as potential structural materials with high damping capacity is the cost per pound. Since cobalt is currently in the $3 to $4 per pound range, the finished cost for wrought cobalt parts can be as high as $5 per pound even if large quantity use were projected. In order to evaluate the potentials offered by iron base alloys as damping materials for structural applications at a lower cost per pound (i.e., $0.50/lb.) several iron - chromium base alloys have been examined.

This work was stimulated by the reports distributed by Toshiba Electric Co. (17) on a proprietary Fe-Cr-Aℓ alloy and the existence of a miscribility gap in the Fe - Cr system shown in Figure 15 just as there is in the Cu - Mn case shown in Figure 13. Although the mechanism responsible for the damping in Fe - Cr - Aℓ has not been established the misicibility gap in both systems is a common feature.

Accordingly, samples of Fe - Cr - Aℓ alloys and Fe - Cr - C alloys corresponding to several commercial steels were prepared and tested. The results are summarized for Samples 117-125 shown in Table 5, and Figures 16 and 17. It was found that the optimum temperature for heat treatment was 800°C (1073°K). Heat treatment at higher temperatures (i.e., above 1000°C) (1273°K) within the gamma loop lead to low damping. This may be related to the transformation structure in the resulting bcc phase following the fcc→bcc transition on cooling. Heat treatment at 600°C (873°K) did not yield results which were as satisfactory as those obtained at 800°C.

Reference to Table 5 shows that attractive damping capacity and yield strength characteristics can be obtained in the 85 w/o Fe - 12 w/o Cr - 3 w/o Aℓ alloy as well as the 86 w/o Fe - 14 w/o Cr - 0.05 w/o C alloy. The latter corresponds in

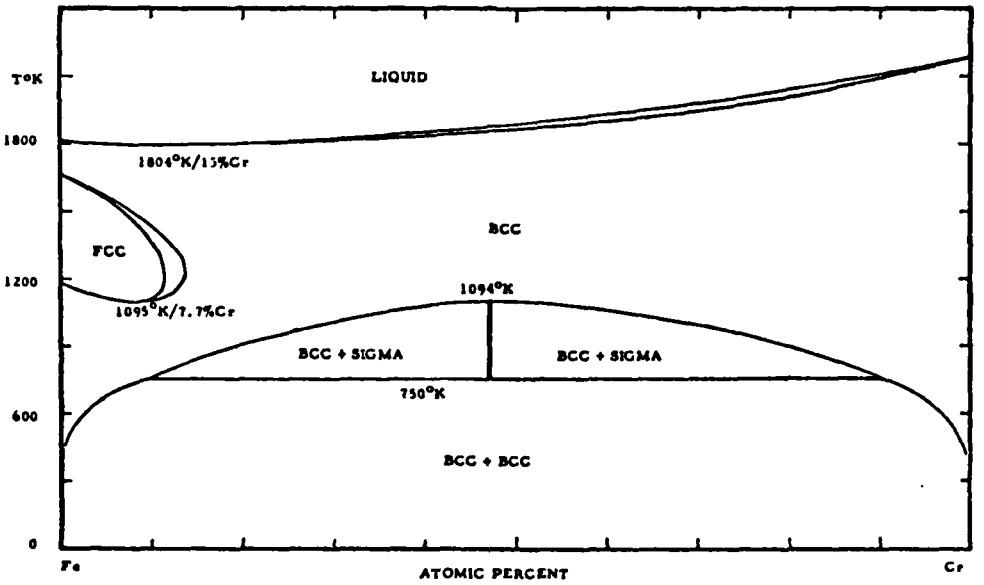

Figure 15. Iron-Chromium Phase Diagram.

TABLE 5

SUMMARY OF 0.2 PERCENT OFFSET YIELD STRENGTH AND RESONANT DWELL DAMPING MEASUREMENTS AT 25°C (Peak Stress 2000 PSI) (SAMPLES WERE MACHINED IN THE COLD WORKED CONDITION AND TESTED DIRECTLY OR ANNEALED AT 800°C OR 1000°C (AN800, AN1000) AND AIR COOLED BEFORE TESTING)

Sample No. Composition (weight percent)	Condition	Resonant Frequency (Hz.)	Dynamical Young's Modulus (PSI x 10^{-6})	Loss Factor	0.2 Percent Offset Yield Strength (PSI)
117-(85Fe-12Cr-3Aℓ)	AN800	258	26.5	0.0360	37900
118-(85Fe-12Cr-3Aℓ)	CW	260	26.6	0.0030	42000
119-(85Fe-12Cr-3Aℓ)	AN600	256	26.4	0.0030	32500
120-(85Fe-12Cr-3Aℓ)	CW	257	26.5	0.0030	39000
121-(88Fe-12Cr-0.12C)	AN800	290	31.8	0.0028	40000
122-(88Fe-12Cr-0.12C)	CW	292	32.2	0.0010	49000
123-(88Fe-12Cr-0.08C)	AN800	288	31.3	0.0042	54000
124-(88Fe-12Cr-0.08C)	CW	290	31.8	0.0015	84000
125-(86Fe-14Cr-0.05C)	AN800	292	32.2	0.0180	42000
126-(86Fe-14Cr-0.05C)	CW	303	34.3	0.0008	49000
TESTED AT A PEAK STRESS OF 500 PSI					
109-(80Co-20Fe)	AN1000	250	24.3	0.0202	17400
TESTED IN A MAGNETIC FIELD UNDER CONDITIONS OF SATURATION					
109-(80Co-20Fe)	AN1000	243	24.0	0.0340	17400
117-(85Fe-12Cr-3Aℓ)	AN800	258	26.5	0.0250	37900
125-(87Fe-13Cr)	AN800	294	32.6	0.0130	42000

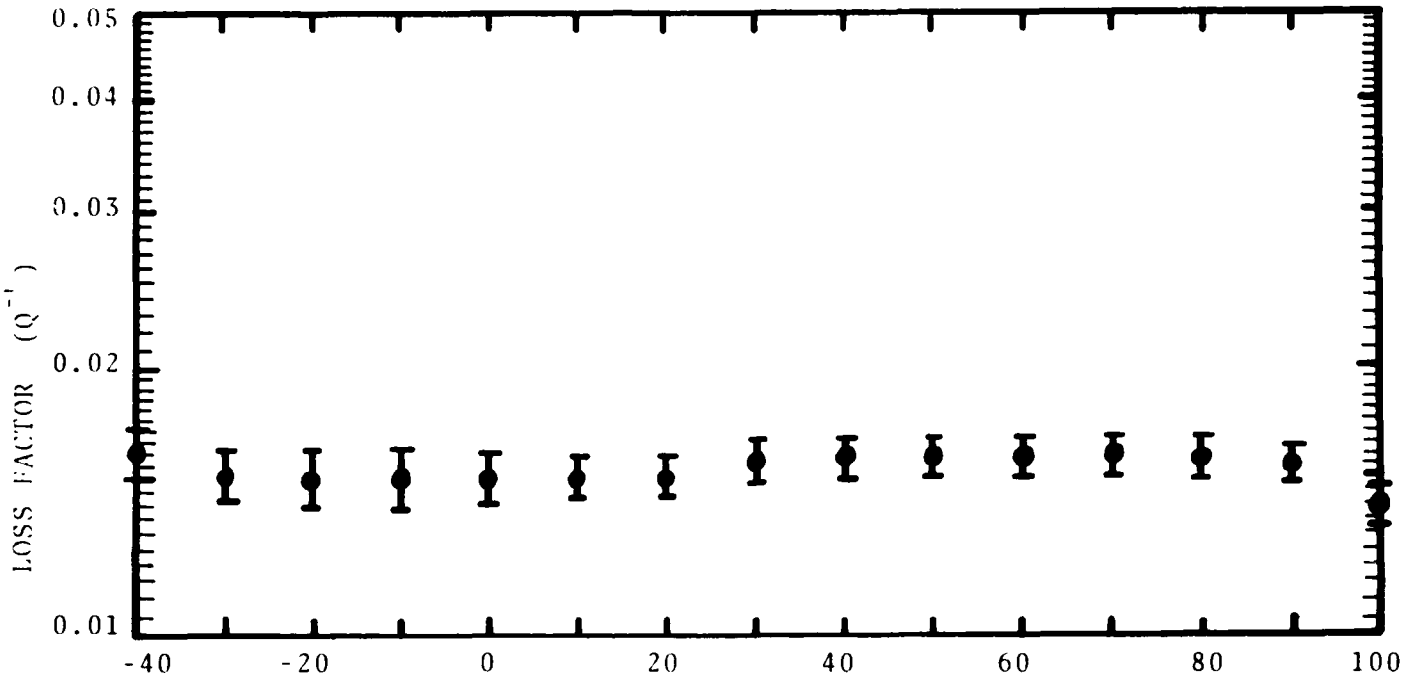

Figure 16. Loss Factor vs. Temperature Curve for a Sample of 85 w/o Fe - 14 w/o Cr - 0.05 w/o C Measured at 290 - 300 Hertz and a Stress of 2000 psi.

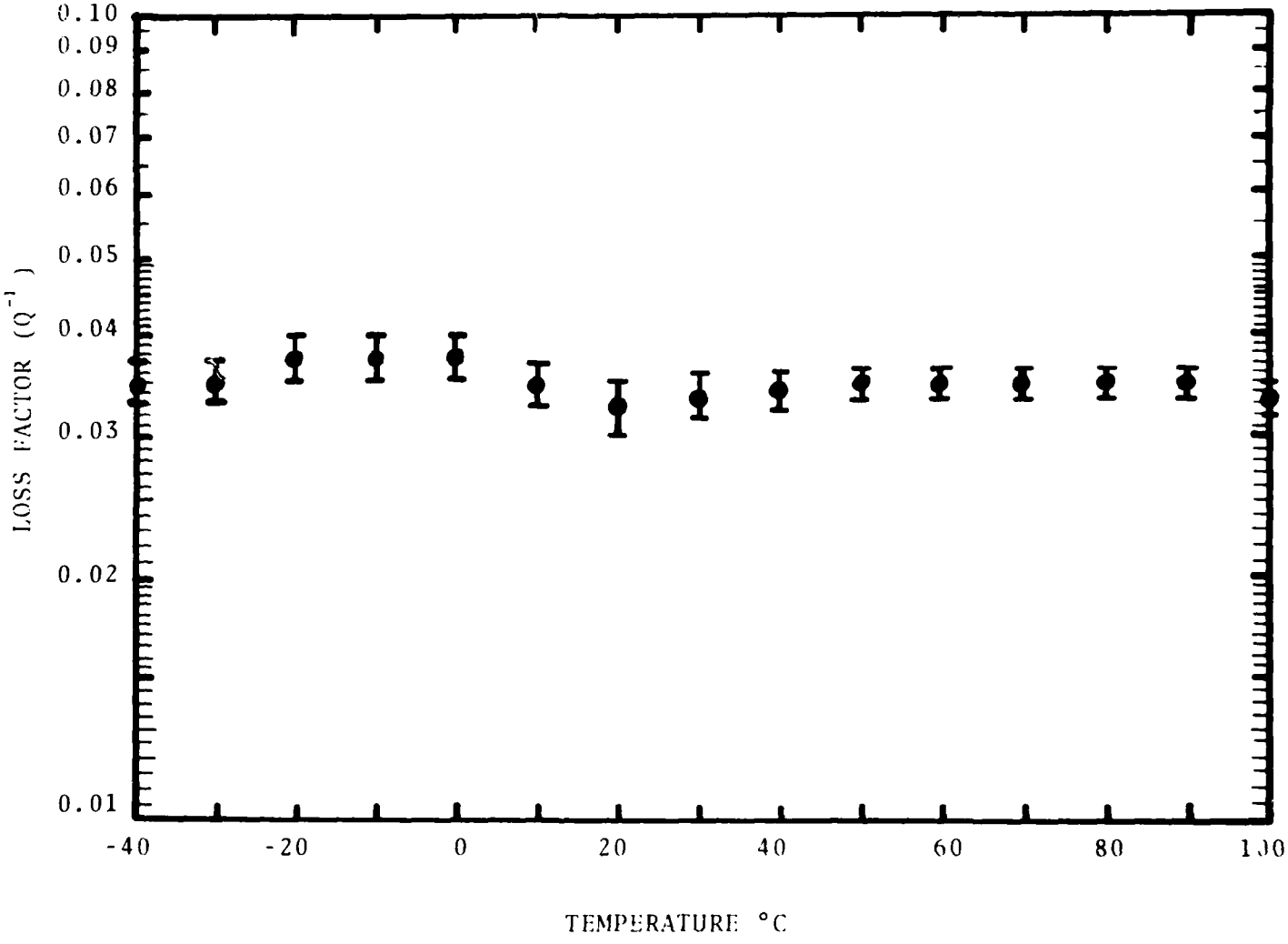

Figure 17. Loss Factor vs. Temperature Curve for a Sample of 85 w/o Fe - 12 w/o Cr - 3 w/o Al measured at 250-260 Hertz and a Stress of 2000 psi.

in composition to type 405 stainless steel (i.e., samples 125, 126). Samples 121, 122, 123 and 124 correspond to types 410 and 403 stainless steel respectively. The results indicate that combinations of 4000 psi yield strength, loss factors of 0.02 - 0.04, good corrosion resistance and a cost per pound of $0.50 - $0.80/lb., can readily be attained in alloys of the iron - chromium system. However, optimization of properties will undoubtedly depend on third alloying element additions as well as heat treatment as indicated by Table 5.

Figures 16 and 17 indicate that the damping is insensitive to changes in temperature up to 100 °C. These results were obtained on samples 125 and 111 which are shown in Figures 16 and 17 respectively. The results of similar studies at Toshiba Electric suggests that the loss factor is insensitive to temperature up to 300°C. Table 5 also contains some results on the 80 w/o Co - 20 W/o Fe alloy at a lower stress (500 psi) as well as the 80 w/o - 20 w/o Fe and the iron - chromium alloys in a saturating field.

The former result at 500 psi indicates a loss factor of about 2% for the Co - Fe alloys as compared with a loss factor of 4% for this alloy at 2000 psi. This is in keeping with the general finding that the loss factor is proportional to stress to the one half power.

Measurement of the loss factor at 2000 psi in a saturating magnetic field indicated at 15% decrease in loss factor for the Co - Fe alloy, while the iron- chrmoium alloys exhibited a decrease in the loss factor of nealy 30%.

IV. CONSIDERATION OF POTENTIAL APPLICATIONS OF HIGH DAMPING ALLOYS.

A survey of potential applications of high damping alloys to problems of noise and vibration control was conducted in order to examine problem areas in military and civilian systems, which could benefit from advances in damping materials technology. Tables 6 and 7 list some of the results of this survey. In this listing, general items and specific applications are noted. Each entry is also accompanied by material properties which are required in addition to damping for the specific application. For the cases listed in Tables 6 and 7, high damping characteristics would be a desirable feature of the metallic component since add-on noise or vibration treatments are inappropriate or too expensive.

In the basis of this survey, it appears that three potential application merit particular consideration. These are ship propellers, body panels of military reconnissence vehicles, engine oil pans, and valve covers. In each case, improvement in the damping properties may be expected to lead to significant reductions of radiated noise and hence, in acoustic detectibility an/or tolerance. In the former application, damped propellers have proven to be effective. The availability of high damping alloys with a known loss factor could lead to propellers with better reliability allowing design for optimized thrust at a lower cost. The benefits of additional damping in materials used for body panels of military reconnaissance vehicles, and for engine components have not yet been quantitatively determined. However, a recently completed model study (18) has demonstrated its significance. Subsequent parts of this section discuss these principal areas of application.

1.0 High Damping Materials For Military Ship Propellers

High damping in some propellers of military vessels is currently acheived through a complicated design involving

TABLE 6

POTENTIAL APPLICATIONS OF HIGH DAMPING ALLOYS IN NOISE CONTROL

ITEM	APPLICATION	PRIMARY PROPERTIES
Propellors	Military Ship Propulsion	Corrosion Resistance Surface Fatigue Strength
Gears	Ship & Helicopter Power Train	Fatigue Strength Stiffness
Hull Plating and Engine Oil Pans and Valve Covers	Military Reconnaissance Vehicles	Formability
Mufflers and Ducts	Air Compressors	Fatigue Strength
Damped Springs & Suspensions	Land Vehicles	Fatigue Strength
Perforated Plates for Test Cells	Engine Test Cells	High Temperature
Cams and Cam Followers Relays & Ratchets	Machinery & Control Systems	Fatigue Strength Stiffness
Machinery Stops	Production Machines Automatic Weapons	Fatigue Strength Stiffness
Saw Blades	Fabrication Machinery	Fatigue Strength Abrasions Resistance
Impact Bits	Jack Hammers	Abrasions Resistance Fatigue
Grinders & Pelletizers	Material Preprocessing (e.g., plastics)	Abrasions Resistance
Wheel Squeal	Rail Vehicle Wheels and Retarders	Abrasion Resistance
Material Transfer & Handling	Food & Chemical Processing	Abrasion Resistance Resistance to Chemicals Formability

TABLE 7

POTENTIAL APPLICATIONS OF HIGH DAMPING ALLOYS IN VIBRATION AND FATIGUE CONTROL

ITEM	APPLICATION	PRIMARY PROPERTIES
VIBRATION CONTROL		
Engine Crank Shafts	Piston Engines	Fatigue
Electronic Chasses	Vehicle-Borne Electronics	Fatigue
Machine Tool Holders	Production Machinery	Strength
Machinery Stops	Production Machinery Automatic Weapons	Stiffness Fatigue Strength
Cam & Cam Followers, Rely & Ratchet Devices	Machinery & Control Systems (e.g., high speed printers)	Fatigue Strength Stiffness
FATIGUE CONTROL		
Turbine Blades	Turbo Machinery	High Temperature Strength Low Density
Aircraft Components	Surface Structures and Equipment Near Engines and Armaments	Fatigue Strength
Light Bulb Filaments	Bulbs for all Vehicles	Luminescence Electrical Resistance High temperature Fatigue Strength
Nuclear Reactor Components	Gas Cooled Reactors	Compatibility with Reactor Environment

composite materials. The levels of damping achieved by this route are satisfactory. Loss factors of the propellers as a vibratory system are not available at this time. However, materials with loss factors of 4% under the required dynamic and static stresses are serious candidates for propeller materials if costs are reasonable and, if other important materials properties are achieved. In particular, any materials which is considered for use must generally meet the requirements of MIL-B-21230, which are as follows: Fatigue Life: 10^8 cycles in salt water at a 9000 psi mean stress, 2700 psi alternating stress. A yield strength of 35000 psi is required and the material must be castable, easily welded, and capable of withstanding chipping and grinding. In addition, it must be machinable so that a 63 micro-inch finish can be acheived. The alloy must be resistant to stress corrosion, cavitation corrosion, and fatigue for long periods of exposure.

Salt water fatigue tests are performed at NSRDC Annapolis. The specimen size required is a 10.5 to 12 inch long bar with a 1" circular cross section. The speciman is cantilevered and point loaded at the free end to produce a peak stress which is increased to 9-13000 psi. Salt water is applied to a 3 inch long section of the bar at the clamped end and a dynamic stress of 2700 psi around the mean is applied for 10^8 cycles at a rate of 1450 cycles per minute. Thus, this test requires approximately fifty days of continous testing. Typically five tests are run, and one control test is run in air. Cavitation corrosion tests are performed by NSROC Annapolis. The test sample required is a 6" x 6" x 1/8" plate.

2. High Damping Material For Armoured Personnel Carriers.

Recent measurements performed by Bolt, Beranek and Newman Inc., under contract No. DAAE07-74-C-0002 on a 1/6 scale dynamic model of an armoured personnel carrier (APC) indicated

that the exterior and interior noise of an APC depends significantly on the damping of the APC hull. The 1/6 scale dynamic model, which is shown in Figures 18-21 has been instrumented in order to provide detailed measurements of interior and exterior radiated noise (18). Although no quantitative measurements were made, it was found that the addition of damping treatment greatly reduced the observed noise.

A high damping metal or alloy could make a contribution here, if it can meet all other requirements for APC hull panels. Foremost, there is "ballistic penetration resistance". Since current hulls are made of 5083 aluminum, any new material would have to provide comparable performance per unit weight. Requirements for hull materials properties are contained in MIL-A-46027 and its Ballistics Acceptance Supplement.

It appears that specific goals for materials loss factor can be determined using the above mentioned scale model. A measurement program could be initiated to determine radiated noise reduction as a function of hull panel loss factor. An upper bound on the useful loss factor will exist, since further damping to reduce noise is not useful once the pause noise contribution is approximately the same as that from other noise sources (e.g., the track). Panels with add-on damping treatment could be utilized in this test.

Alternatively, the alloys discussed in Sections I and II could be tested directly on the 1/6 scale model to carry out comparative measurements of radiated power. In order to carry out such a test, eleven plates of the alloys must be fabricated and machined to fit the model. Comparative measurements of the damping alloys vs. aluminum, for both interior and exterior noise could then be made for the model over a range of speeds. The specific plate sizes in 1/4" thick gauge are 11" x 18", 10" x 16", 16" x17", 9" x 16", 4" x 11", 5" x 21" (2) and 6" x 21" (2). Finally, two plates measuring 1/10" x 4" x 21" are required.

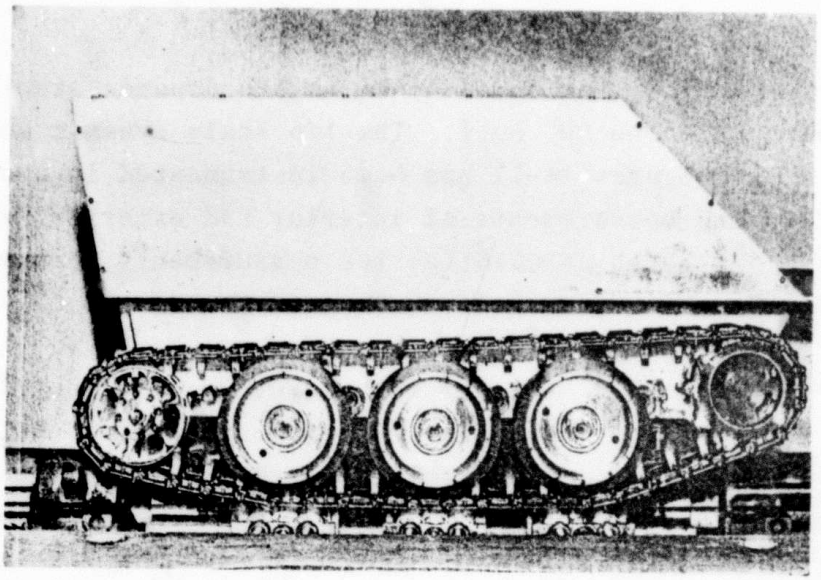

Figure 18. Side View of 1/6 Scale Model of Armoured Personnel Carrier (Courtesy of Bolt, Beranek, Newman Contract DAAE07-74-C-0022).

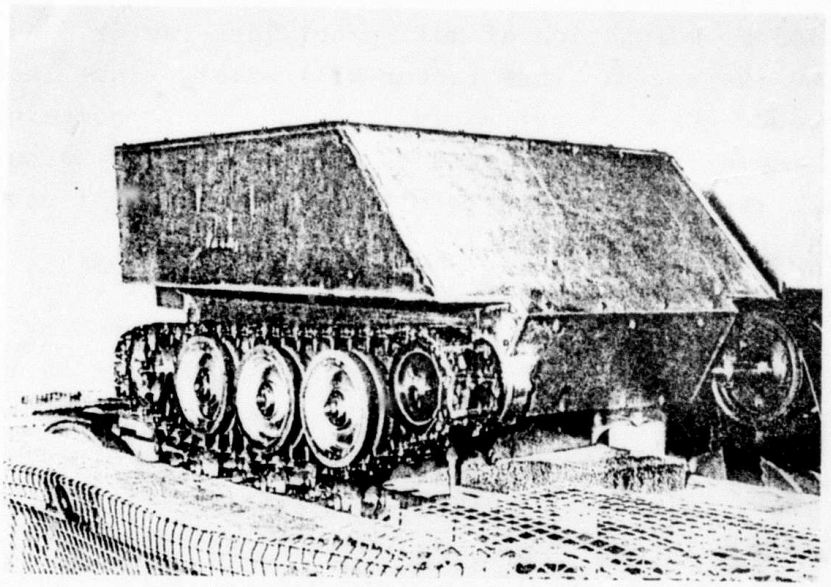

Figure 19. Front View of 1/6 Scale Dynamic Model.

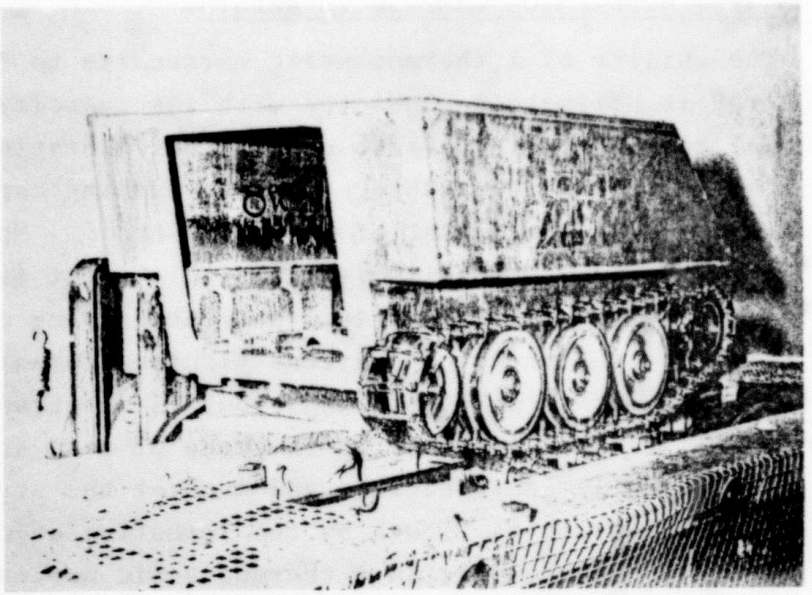

Figure 20. Rear View of 1/6 Scale Dynamic Model of Armoured Personnel Carrier (Courtesy of Bolt, Beranek, Newman Contract DAAE07-74-C-002).

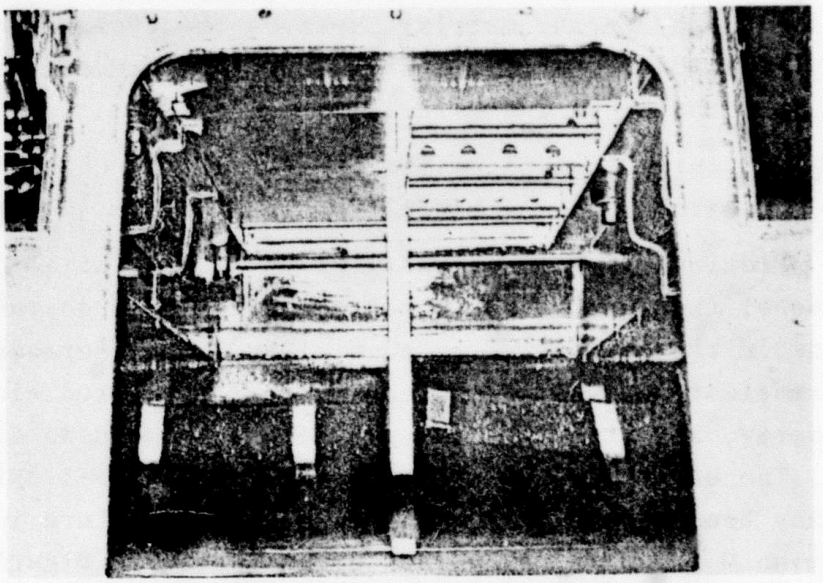

Figure 21. Close-up of 1/6 Scale Model Rear View.

V. MECHANISTIC STUDIES OF DAMPING IN ALLOYS.

The ability of a thermoelastic martensite to "store" elastic energy is ultimately connected with the capacity of that same material to continually absorb or damp out vibrational energy in a materials is nonrepeatable, then the damping capacity will deteriorate with the amount of energy absorbed. However, if the energy-absorbing mechanism is repeatable, that is, it is able to return to its original state, then the damping capacity will not readily deteriorate. A martensitic transformation can be used to absorb mechanical vibrations, but if the transformation is nonthermoelastic (such as in the case of most steels), then it is essentially nonrepeatable and much of the strain energy of the transformation is "lost" by the formation of defects in the matrix. The strain energy in a thermoelastic martensitic transformation, however, is stored elastically in the matrix. This elastic strain energy is recoverable, and can aid the reverse transformation. Increasing the thermoelasticity of a martensitic transformation (by increasing the amount of recoverable strain energy in the matrix) improves the cyclability of the transformation and thus promotes the long-term efficiency of energy absorption in the material.

1. Investigation of the Transformation Characteristics in Cu-Aℓ-Ni alloys.

Previous investigation (1,2) of Cu-Aℓ-Ni alloy has shown some of the effects of stored elastic energy on the thermoelastic transformation in that alloy. The thermodynamics of a thermoelastic system are also affected by stored elastic strain energy, and study of this problem has been undertaken.

The electrical resistivity of a Cu-14.0Aℓ-3.0Ni single crystal has been measured as a function of temperature in order to determine M_s, M_f, A_s, A_f. The curve plotted in Figure 22A is not the same as that presented in reference (2). Although the

specimens were taken from the same (large) single crystal, the present sample was heat treated and quenches separately from the one (same composition) previously treated. Even the small difference in quenching rates of the two samples for the solutionizing temperature of 950°C can change the degree of long-range order sufficiently to have a fairly large effect on the transformation temperatures.

The resistivity versus temperature curve of the single-crystal specimen (Figure 22A) shows M_s to be -1°C and A_f to be 37°C. The temperatures for M_f and A_s cannot be determined so accurately from the curve because of the relatively gradual changes in slope near both M_f and A_s. Certainly the bulk (greater the 90%) of the transformation has been completed by -5°C on cooling and similarly the reversion is underway between 20 and 25°C on heating. It is important to note, however, that the temperatures of importance for present purposes (i.e. M_s and A_f) can be determined quite precisely from the resistivity curves.

The single crystal (with resistivity leads and thermocouple still attached) was cleaned and a thin layer (less than 0.001 in. thick as measured by a micrometer) of Ni was electrolytically plated on the specimen. The electrical resistivity was then measured as a function of temperature (Figure 22B). The M_s has been depressed to approximately -10°C (as compared to the M_s of -1°C) for the unplated specimen. The A_f, however, remained at 37°C. The M_f and A_s values are less easily defined; that is the portion of the curve that would indicate M_f on cooling has become more rounded off than it was for the nonplated sample. This is also true for the portion of the heating curve (near 20°C) which is used to yield the (approximate) value for A_s. The increase in "blurring" of M_f and A_s over what it was for the nonplated sample is probably due to the reduced size which the initially-formed martensitic plates can grow to (because of the constraints imposed by the Ni-plating). The reduced size of the

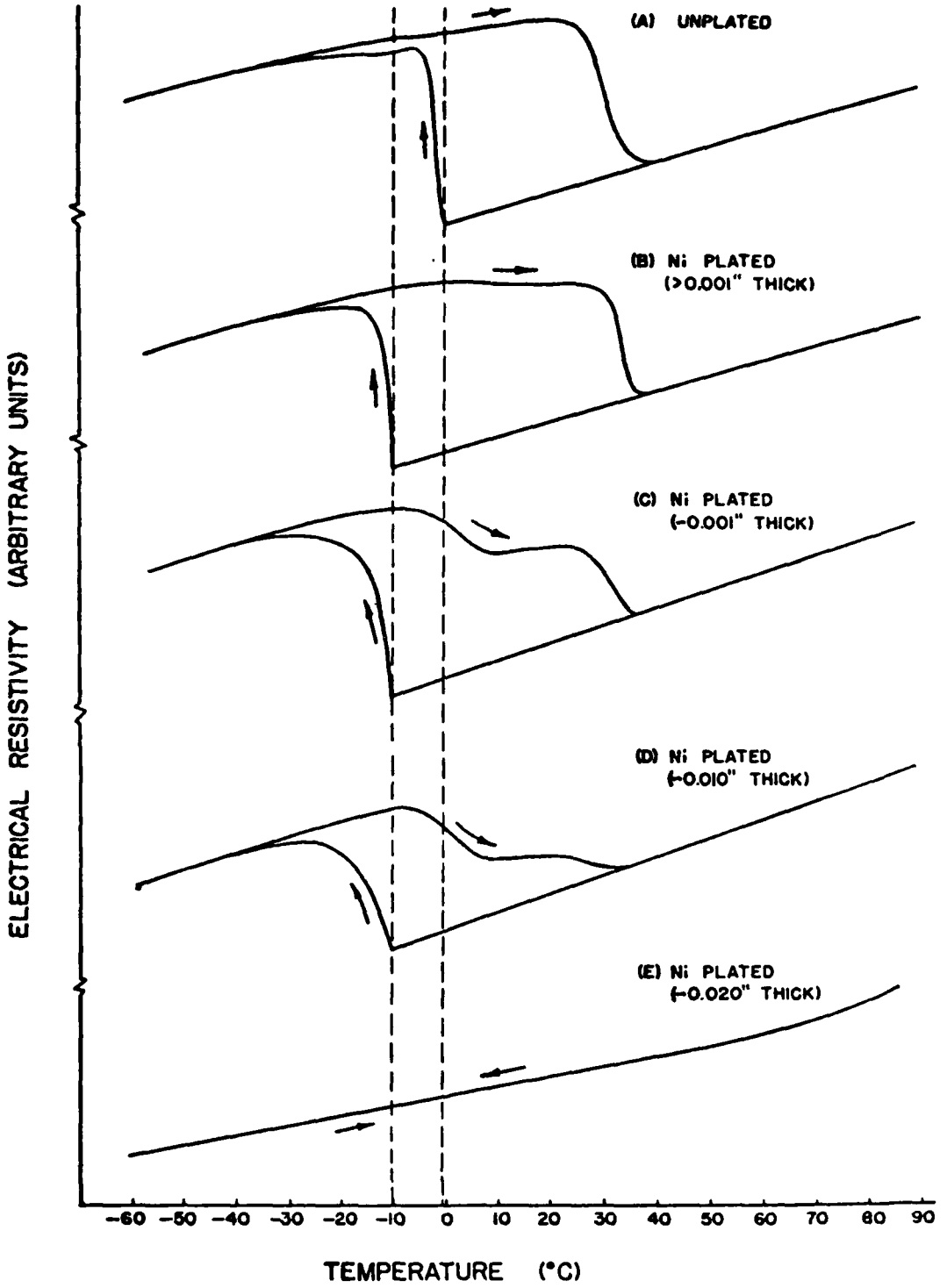

Figure 22. Transformation Hysteresis Curves for a Cu-14.0Aℓ-3.0Ni Single Crystal with Different Thickness of Ni-Plating on the Specimen Surface.

first-formed plates results in a larger volume fraction of the sample that must be transformed by still smaller plates "filling in" between the initial plates. These small plates require a larger undercooling in order to form because of the elastic strain energy stored in the system by the more complex geometry of the aggregate of plates.

Another layer of Ni was added to the surface of the specimen and the resistivity versus temperature was again measured (Figure 22C). The M_s remains unchanged at -10°C while A_f has been lowered slightly to about 34°C (from the previous value of 37°C). The "blurring" of the M_f portion of the curve (around -20°C on cooling) is greater than in the previous runs. On heating, the resistivity displays a dip that starts at about -10°C. When more Ni is added to the plating (about 0.010 inch), the resistivity curve (Figure 22D) shows and enhancement of the effects exhibited by the curve of Figure 1c. In other words, M_s and A_f remain approximately constant at -10°C and 34°C respectively, but the curve (on cooling) rounds off even more in the vicinity of M_f and the dip on heating (starting at about -10°C) becomes more pronounced.

A thick Ni-layer was finally applied to the surface and the resulting resistivity is shown in Figure 22E. This final Ni-plating was about 20 mils thick. The resistivity curve was nearly a straight line, and did not indicate any transformation occurring in the temperature range observed. Samples with Ni-plating of thickness intermediate between those reported in Figures 22D and 22E showed basically the same behavior as the curve in figure 22D.

The curves in Figure 22 represent rather unusual behavior for thermoelastic martensitic material; this behavior as presently understood will be described below. The first Ni-plating seems to have depressed M_s by suppressing the surface nucleation of the martensite (i.e. the free surface is, in effect, removed

by the Ni-plating). The M_f and A_s are less well defined because of the increased number of smaller plates (which previousely were able to grow to almost the entire volume of the specimen). As the Ni-plating is increased in thickness, the M_s and A_f remain relatively unchanged. The M_f portion of the curve becomes increasingly rounded-off, indicating that a larger part of the sample volume is being taken up by smaller plates. The transformation is thus rendered more thermoelastic -- that is, the Ni-plating causes a greater amount of elastic strain energy to be stored in the matrix and this has the effect of making the transformation of the single crystal occur via a greater number of plates and variants than was previously observed in the unplated condition. The elastic strain energy stored in the Ni-plated smaple can be used to promote the reverse transformation on heating -- this seems to be the cause of the early dip in the heating curve, which increases in magnitude as the thickness of the Ni-plating is increased. If this is the case, then at some Ni-plating thickness, the amount of strain energy stored in the Ni-plated sample should be sufficient to cause the reversion of the sample to be complete before the A_f of the unplated sample. This behavior was not reached in the present set of experiments, the most probable reason being that the conductivity of the thick Ni-plating become sufficiently large to obscure any resistivity changes due to the transformation itself.

Subsequently, the specimen with the thick Ni-plating was electropolished to remove the Ni. The resistivity curve of this sample (unplated) was then remeasured and is shown in Fingure 23A. The M_s increased to -2°C (compared to -1°C for the unplated specimen). This demonstrates that the effect of the Ni-plating is reversible and that removing the Ni-plating causes the return of M_s to -10°C, with little or no influence on the A_f.

The previous progress report (2) contained initial calorimetry data which has now been remeasured because of the possibility that some of the transformation strain energy could have been stored in the holding pans in which the various Cu-Aℓ-Ni samples were sealed. The experiments were repeated with the same samples contained in holders which could not confine them (and thus not store any transformation strain energy). The values from the new experiments are listed in Table 8a, and can be compared with the values previously reported (see Table 8b). The agreement is good for all the single-crystal values of ΔH (cooling). The ΔH (cooling) values for the polycrystalline samples increased slightly, indicating a decrease in elastic energy stored during the transformation. The agreement between the values of ΔH (heating) is not as good -- the reason is primarily due to the quite subjective nature of deciding where the peaks begin and end during the reverse transformaion. Thus, the value of ΔH (heating) is to ascertain whether the values are reasonable close to the ΔH (cooling) values. The single crystal (32.8 mg) again exhibited a ΔH curve on cooling which indicated that it was (as closely as can be determined in the calorimeter) a single-interface transformation (the sample exhibited the same sharp transformation curve even at cooling rates as low as 0.31° K/min). The other samples exhibited curves which indicated that they did not transform via a single interface. A difference on the order of 10 cal/mole is found between the two cases (both single crystal and polycrystal samples). Hence, the measurements indicate that the stored elastic strain energy contribution to the enthalpy in multiple interface transformations (in samples of this size) is on the order of 10 cal/mole. This difference may, however, be significantly larger in more massive and fine-grained specimens where the strain energy from the transformation can be more efficiently stored.

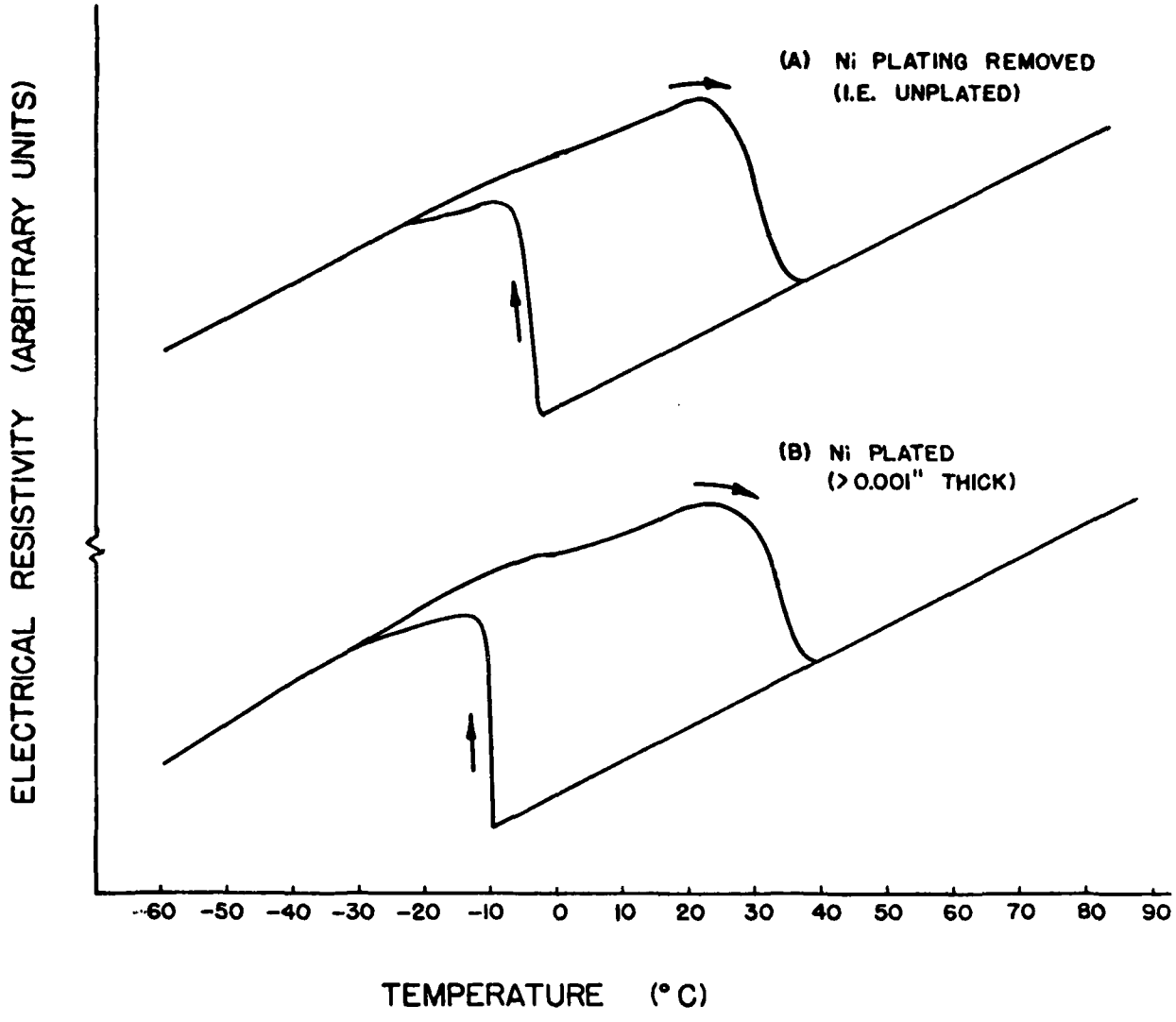

Figure 23. Transformation Hysteresis Curves for a Cu-14.0Aℓ-3.0Ni Single Crystal with (a) Ni-Plating Removed and (b) a Thin Ni-Plating Reapplied.

TABLE 8

TOTAL ENTHALPY CHANGE IN SINGLE-CRYSTAL AND POLYCRYSTALLINE SAMPLES OF Cu - 14.0Aℓ - 30Ni AS MEASURED BY A SCANNING DIFFERENTIAL CALORIMETER (cooling and heating rates or 40° K/min)

(a) NONCONFINING SAMPLE HOLDERS

Sample	$\Delta H_{cooling}$ cal/mole	$\Delta H_{heating}$ cal/mole
Single Crystal (32.8 mg) [single interface]	123	-128
Single Crystal (71.0 mg)	113	-120
Single Crystal (85.8 mg)	106	-121
Polycrystal (37.7 mg)	113	-120
Polycrystal (93.2 mg)	113	-112

(b) CONFINING SAMPLE HOLDER (from previous report[2])

Sample	$\Delta H_{cooling}$ cal/mole	$\Delta H_{cooling}$ cal/mole
Single Crystal (32.8 mg) [single interface]	124	-120
Single Crystal (71.0 mg)	115	-123
Single Crystal (85.8 mg)	107	-116
Polycrystal (37.7 mg)	109	-111
Polycrystal (93.2 mg)	108	-112

The absolute magnitude of the nonchemical enthalpy can be increased if the difference between T_o (the temperature where the chemical free-energy change is zero) and the average transformation temperature is increased, and this can be accomplished by making the sample polycrystalline (see reference (2)). It has been shown previously that a thin Ni-plating on the surface of the Cu-Aℓ-Ni sample can depress the M_s by several degrees. This depression M_s and also in the average transformation temperature should lead to a decrease in the observed ΔH cooling of a Ni-plated sample (this will be more fully explained later in the text).

The samples previously examined in the unplated state were lightly chemically polished, weighed and then electrolytically plated with a thin layer on Ni. The samples on which the Ni-plating kept its integrity (after the samples were transformed and reverted) had a M_s that was significantly depressed. The value of ΔH cooling was also decreased as shown in Table 9. Further, the single crystal (32.8 mg), which had previously (when unplated) exhibited a single-interface transformation, displayed a ΔH transformation curve with much structure after the sample was Ni-plated. This indicates a change from a single-interface transformation to a multiple-interface transformation in the same sample. Typical ΔH (cooling) transformation curves are shown in Figure 3 for the Ni-plated and unplated samples. The ΔH (cooling) value was decreased from 123 cal/mole (for the single-interface transformation in the single crystal 32.8 mg) to 101 cal/mole for the Ni-plated sample (which had a multiple-interface transformation). The ΔH (cooling) values of the polycrystalline samples (37.3 mg and 89.2 mg) were decreased from 113 and 113 cal/mole to values of 101 and 105 cal/mole respectively for the Ni-plated specimens.

The transformation of the nonplated 32.8 mg. single-crystal sample seems to have occurred by a single-interface mechanism.

A basic thermodynamic relationship for a thermoelastic transformation is given by

$$\Delta G^{\beta_1 \rightarrow \gamma'}_{total} = \Delta G^{\beta_1 \rightarrow \gamma'}_{chem} + \Delta G^{\beta_1 \rightarrow \gamma'}_{nonchem} \qquad (2)$$

where the $\Delta G^{\beta_1 \rightarrow \gamma'}_{total}$ is the total Gibbs free-energy change accompanying the $\beta_1 \rightarrow \gamma'$ transformation while $\Delta G^{\beta_1 \rightarrow \gamma'}_{chem}$ is the chemical portion and $\Delta G^{\beta_1 \rightarrow \gamma'}_{nonchem}$ is the nonchemical portion of the total free-energy change. $\Delta G^{\beta_1 \rightarrow \gamma'}_{nonchem}$ consists mainly of elastic strain-energy contributions in thermoelastic martensite but can have contributions from interfacial energies resulting from the production of interfaces, etc. If the (normally) thermoelastic alloys transforms to martensite by a single-interface transformation, the the nonchemical term involved in equation (2) is eliminated. There is then essentially no nonchemical term in the free-energy expression. Correspondingly, the enthalpy of the transformation is entirely a chemical enthalpy in a single-interface transformation. The enthalpy measured for the single-interface transformation of Cu-14.0Aℓ-3.0Ni indicates that $\Delta H^{\beta_1 \rightarrow \gamma'}_{chem} = 123$ cal/mole. Therefore, since $\Delta G^{\beta_1 \rightarrow \gamma'}_{total} = \Delta G^{\beta_1 \rightarrow \gamma'}_{chem} = 0$ at T_o (for the single-interface transformation):

$$\Delta S^{\beta_1 \rightarrow \gamma'}_{chem} = \frac{\Delta H^{\beta_1 \rightarrow \gamma'}_{chem}}{T_o} \qquad (3)$$

where $\Delta S^{\beta_1 \rightarrow \gamma'}_{chem}$ is the chemical entropy change for the $\beta_1 \rightarrow \gamma'$ transformation. The value of T_o is taken to $(A_f - M_s)/2$ (for a single crystal specimen -- see reference (2) for details), where A_f and M_s are obtained from the calorimeter curves. For the single crystals (either single interface or multiple interface), the T_o is 42°C and M_s and A_s are 14°C and 70°C respectively. The value for $\Delta S^{\beta_1 \rightarrow \gamma'}_{chem}$ can then be calculated as 0.39 cal/mole °K. The chemical free-energy

TABLE 9

TOTAL ENTHALPY CHANGE IN NON-PLATED AND NICKEL PLATED SAMPLES OF Cu - 14.0Aℓ - 3.0Ni MEASURED BY A SCANNING DIFFERENTIAL CALORIMETER (cooling rate of 40° K/min.)

Sample	H cooling (cal/mole)	M_s (°K)	$\bar{T}$ °K
Single Crystal (32.8 mg)			
Unplated	123	287	∿285
Ni-plated	101	281	∿272
Polycrystal (37.3 mg)			
Unplated	113	274	∿270
Ni-Plated	101	257	∿255
Polycrystal (93.2 mg)			
Unplated	113	270	∿265
Ni-Plated	105	257	∿254

* $\bar{T}$ is the average transformation temperature.

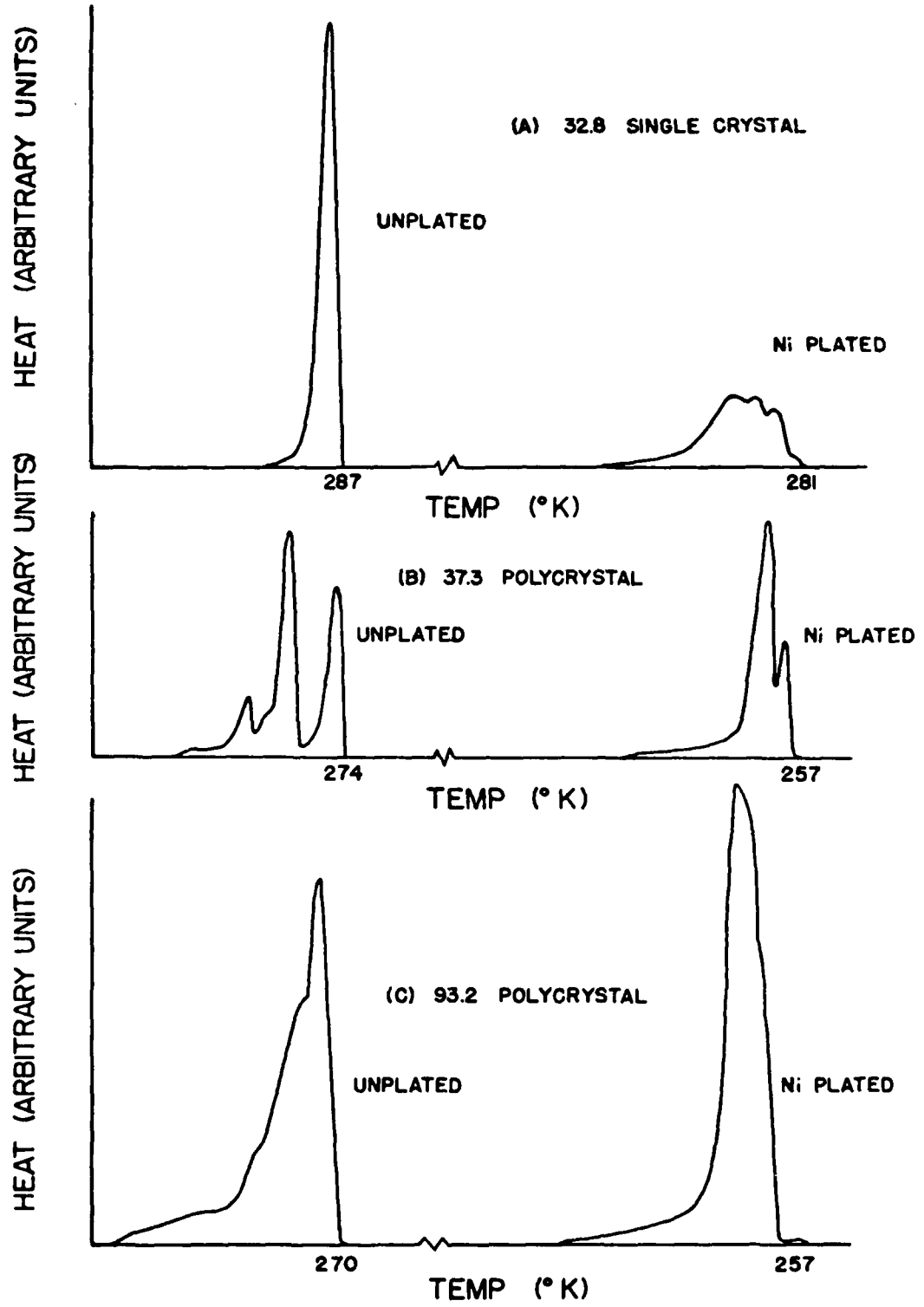

Figure 24. Scanning Differential Calorimeter Curves for Various Cu-14.0Aℓ-3.0Ni Samples in Both the Unplated and Ni-Plated Conditions.

change at M_s for the single-interface transformation is given by:

$$\Delta G_{M_s}^{\beta_1 \rightarrow \gamma'} = -(\Delta S_{chem}^{\beta_1 \rightarrow \gamma'})(T_o - M_s). \qquad (4)$$

and $G_{M_s}^{\beta_1 \rightarrow \gamma'}$ is -10.9 cal/mole (i.e. the chemical driving force is equal to 10.9 cal/mole).

The concept of thermoelasticity involves the condition that the chemical and elastic free energies should be similare in magnitude, and so during martensite growth:

$$\Delta G_{chem} + n\Delta G_{elas} = 0$$

where n is a small number (esitmated to be close to 2 by Olson and Cohen Scripta Met., Nov. 1975). A consequence of this condition is that, as the transformation occurs farther from T_o (i.e. at larger supercoolings), the chemical driving force becomes larger and thus the magnitude of ΔG_{elas} also becomes increasingly large. Because

$$\Delta H_{total} = \Delta H_{chem} + \Delta H_{elas} = \Delta H_{measured}$$

and ΔH_{chem} and ΔH_{elas} have opposite signs, the effect of having the transformation occur at greater supercoolings is to cause the total measured ΔH to become smaller. This has been shown to be the case for the polycrystalline samples which were Ni-plated where the average transformation temperature is lowered significantly.

2. Studies of Cobalt-Iron Alloys

Some micrographs of the 80Co-20Fe alloy are given in Figures 25 through 30. The starting material was a rod which

had been swaged to about 60% of its starting diameter. The microstructure is shown in Figure 25. Two samples were then encapsulated in vycor and heat treated at 1000°C for one hour -- one sample was water quenched (capsule was broken), and the other was air cooled in the capsule. Micrographs are shown in Figures 26 and 27. They indicate that there was (1) no martensite formation on being cooled to room temperature, and (2) no martensite formed as a result of the polishing. Further cooling in liquid nitrogen also gave no evidence of any phase transformation occurring in either the water-quenched or slowly-cooled samples.

Figure 26a shows an area of the sample which underwent considerable grain growth during heat treatment, whereas 26b is another section of the same surface in which a smaller amount of grain growth was observed. The microstructure of the air-cooled (encapsulated) sample is shown in Figure 27. Again there were areas with a large amount of grain growth (Figure 27a) and other areas where the grain growth was significantly smaller (Figure 27b).

In view of the possibility that magnetic domain wall motion may contribute to damping capacity in Fe-Co alloys, the magnetic domain structure of alloy 402 was investigated using a colloidal suspension of magnetic particles. As a point of reference, Figure 28 illustrates the domain structure of Fe-4% Si transformer sheet. The direction of easy magnetization is marked; the domain walls in the largest grain lie parallel to the easy-magnetization direction. The domains in the smaller grain shown are more-or-less randomly oriented. Figure 29 illustrates the domain pattern associated with the water-quenched Co-Fe, and Figure 30 the domain structure after air cooling. The domain size of the water-quenched sample seems to be significantly larger than that of the air-cooled sample. Further investigations into the microstructure of

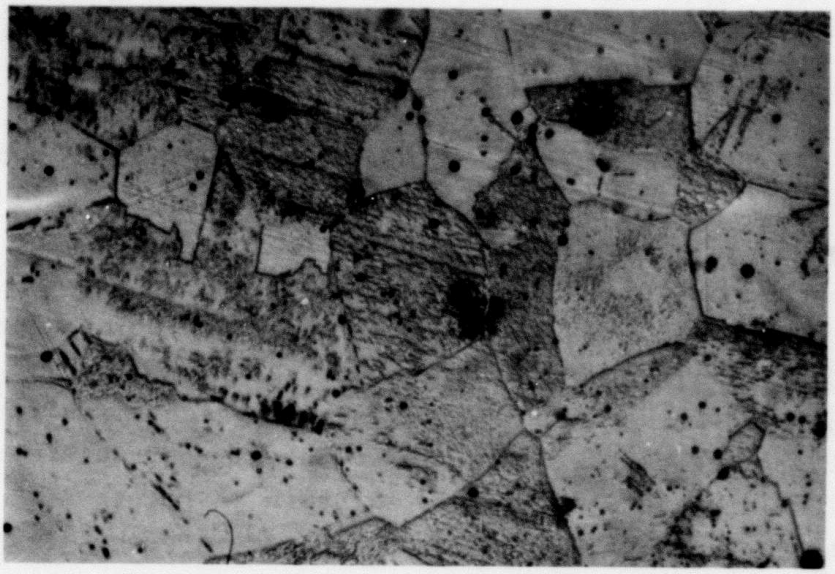

Figure 25. Structure of Heavily Swaged 80Co-20Fe (200x).

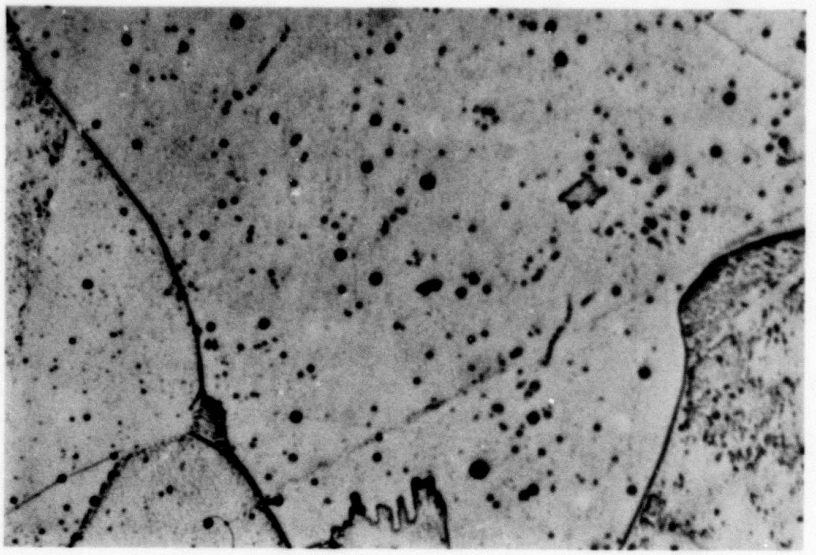

(a)

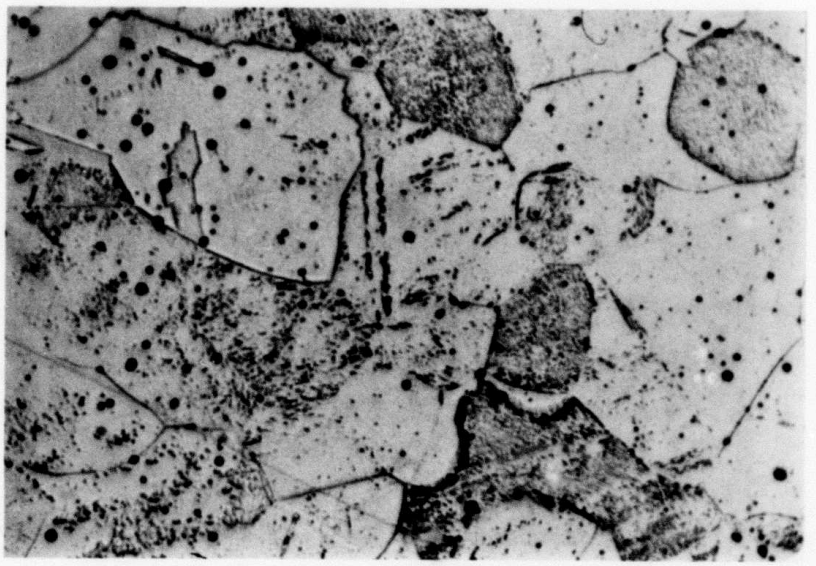

(b)

Figure 26. (a) Grain Growth of 80Co-20Fe Annealed One Hour at 1000°C and Water Quenches (200x).

(b) Area of Same Sample Showing Little Grain Growth (200x).

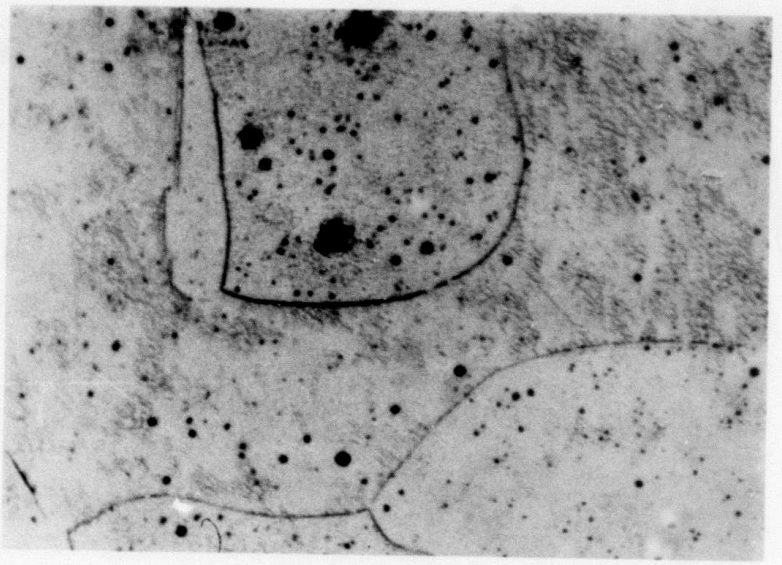

(a)

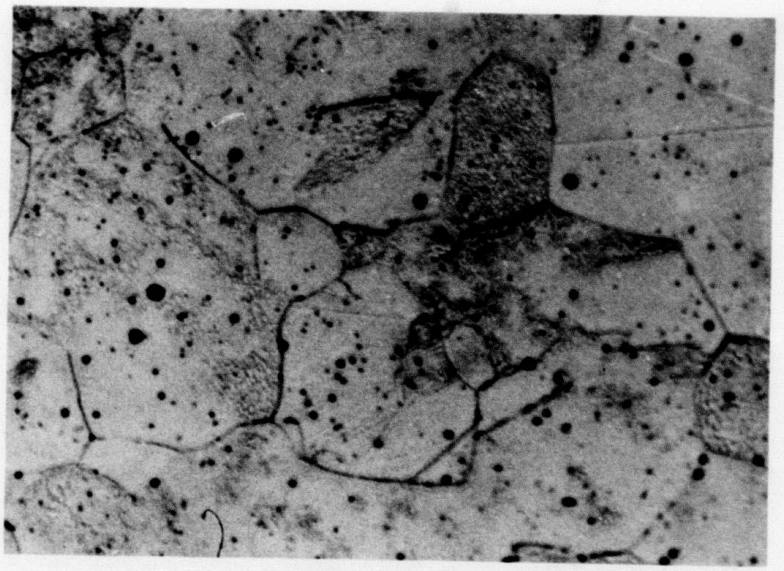

(b)

Figure 27. (a) Grain Growth of 80Co-20Fe Annealed One Hour at 1000°C and Air Cooled (in Vycor Capsule) (200x).

(b) Area of Same Sample Showing Little Grain Growth (200x).

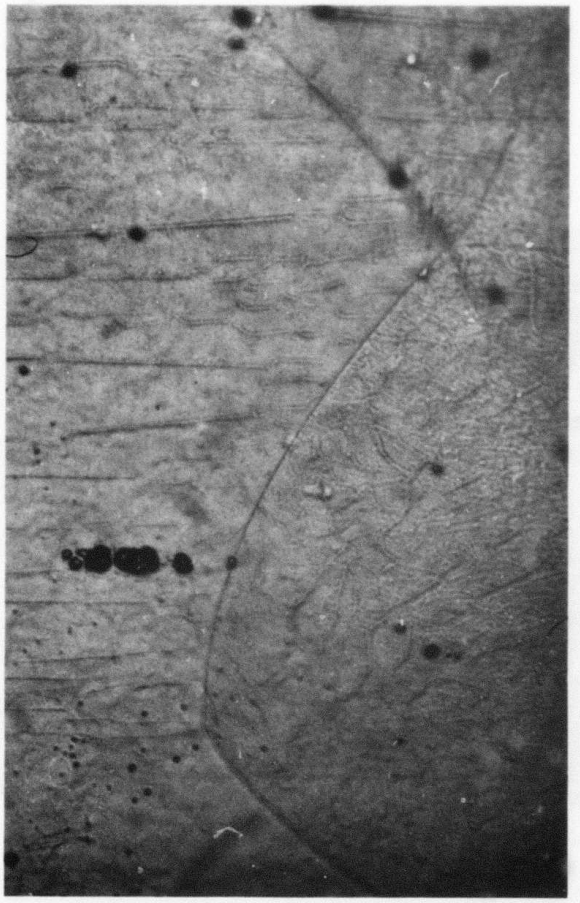

Figure 28. Magnetic Domain Pattern of Fe-4%Si Transfomer Sheet (200x).

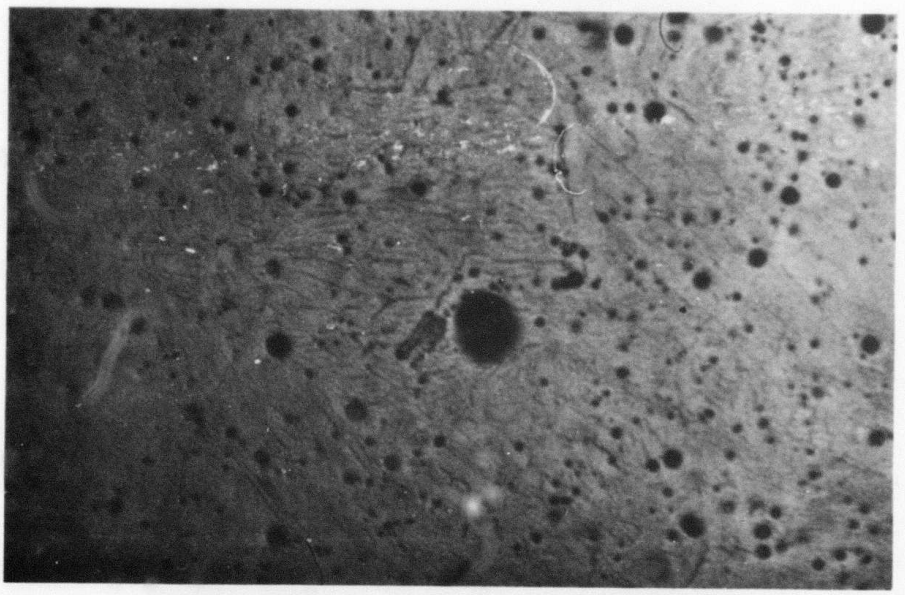

Figure 29. Magnetic Domain Pattern of 80Co-20Fe Annealed at 1000°C for One Hour and Water Quenched (200x).

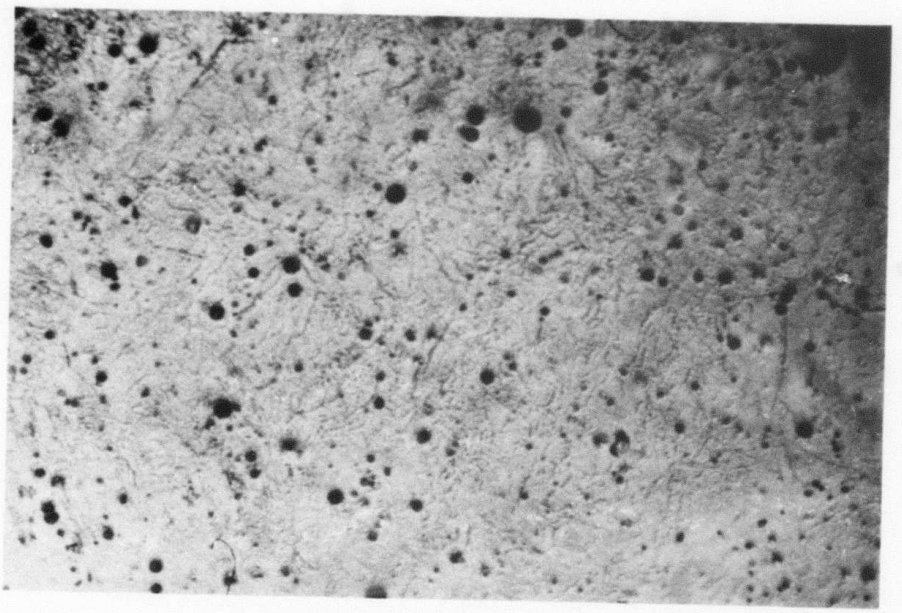

Figure 30. Magnetic Domain Pattern of 80Co-20Fe Annealed at 1000°C for One Hour and Air Cooled (in Vycor Capsule) (200x).

this alloy is continuing, with interest being directed toward (1) improving the quality of the surface of the metallographic specimen, and (2) preparing specimens for transmission electron microscopy.

REFERENCES

1. L. Kaufman, S. A. Kulin and P. P. Neshe, "Noise Abatement and Internal Vibrational Absorption in Potential Structural Materials," AMMRC CTR 75-4, Contract DAAG46-74-C-0048, ARPA Order 2555, March 1975, ManLabs, Inc., Cambridge, Massachusetts 02139.

2. L. Kaufman, S. A. Kulin and P. P. Neshe, "Noise Abatement and Internal Vibrational Absorption in Potential Structural Materials," AMMRC CTR 75-4, Contract DAAG46-74-C-0048, ARPA Order 2555, Sept. 1975, ManLabs, Inc., Cambridge, Massachusetts 02139.

3. A. Cochardt, Tr. A.I.M.E. (1956) 206 1295.

4. A. Cochardt, Magnetic Properties of Metals and Alloys, A.S.M., Cleveland (1959) 251-279.

5. J. C. Fister and S. Shapiro, "Improved High Damping Copper-Base Alloys," International Copper Research Association Project 221, Final Report, September 1974, Olin Metals Research Laboratories, New Haven, Connecticut 06504.

6. J. Perkins, G. R. Edwards and N. Hills, "Materials Approaches to Ship Silencing," June 1974, NPS-59Ps74061, Naval Post Graduate School, Monterey, California.

7. J. F. Nachman, J. C. Napier and A. N. Hammer, "Development of Cu-Mn Base Alloys with High Damping Properties," International Copper Research Association Report No. 152, Final Report, March 1970, Solar Division, International Harvester Corporation, San Diego, California 92112.

8. J. F. Nachman, J. C. Napier and A. N. Hammer, "Development of Cu-Mn Base Alloys with High Damping Properties," International Copper Research Association Project No. 152A, Final Report, March 1971, Solar Division, International Harvester Corporation, San Diego, California 92112.

9. L. Kaufman and H. Nesor, Zeit. Metallkunde (1973) 74 249.

10. K. C. Mills, M. J. Richardson and P. J. Spencer, "Thermodynamic Properties and Phase Diagram of the Fe-Co and Ni-Pt Systems," Faraday Soc. Symposium (In Press).

11. H. Schumann, "Cobalt," (1968) 40 156.

12. U. Hashimoto, J. Japanese Inst. of Metals (1937) 1 177.

13. K. Ishida and T. Nishizawa, Tr. Jap. Inst. of Metals (1974) 15 225.

14. L. Kaufman, Metallurgical Transactions (1969) 245 91.

15. J. M. Vitek and H. Warlimont (1975) (Submitted for publication in Metal Science).

16. Ye. Z. Vintaykin, D. F. Litvin and V. A. Udorenko, Fiz. Metal. Metall., 37 no. 6, 1974, 1228.

17. Toshiba Electric Co.,R and D Center, Kawasaki City, Kanagawa, 210 Japan.

18. T.R. Norris "Tracked Vehicles: Model Study on the Effect of Track Parameter Changes on the Acoustic Signature, Seismic Signature and Interior Noise" Bolt, Beranek and Newman Inc., Report No. 3031, submitted to U.S. Army Tank-Automotive Command, Warren Michigan (1975) (Contract DAAE07-74-C-0002).

DISTRIBUTION LIST

No. of Copies	To
1	Office of the Director, Defense Research and Engineering, The Pentagon, Washington, D. C. 20301
12	Commander, Defense Documentation Center, Cameron Station, Building 5, 5010 Duke Street, Alexandria, Virginia 22314
1	Metals and Ceramics Information Center, Battelle Memorial Institute, 505 King Avenue, Columbus, Ohio 43201
	Chief of Research and Development, Department of the Army, Washington, D. C. 20310
2	ATTN: Physical and Engineering Sciences Division
	Commander, Army Research Office, P. O. Box 12211, Research Triangle Park, North Carolina 27709
1	ATTN: Information Processing Office
	Commander, U. S. Army Materiel Development and Readiness Command, 5001 Eisenhower Avenue, Alexandria, Virginia 22333
1	ATTN: DRCDE-TC
	Commander, U. S. Army Electronics Command, Fort Monmouth, New Jersey 07703
1	ATTN: DRSEL-GG-DD
1	DRSEL-GG-DM
	Commander, U. S. Army Missile Command, Redstone Arsenal, Alabama 35809
1	ATTN: Technical Library
1	DRSMI-RSM, Mr. E. J. Wheelahan
	Commander, U. S. Army Satellite Communications Agency, Fort Monmouth, New Jersey 07703
1	ATTN: Technical Document Center
	Commander, U. S. Army Tank-Automotive Development Center, Warren, Michigan 48090
2	ATTN: DRDTA, Research Library Branch
	Commander, U. S. Army Armament Command, Rock Island, Illinois 61201
2	ATTN: Technical Library
	Commander, White Sands Missile Range, New Mexico 88002
1	ATTN: STEWS-WS-VT
	Commander, Aberdeen Proving Ground, Maryland 21005
1	ATTN: STEAP-TL, Bldg. 305

No. of Copies	To
	Commander, Frankford Arsenal, Philadelphia, Pennsylvania 19137
1	ATTN: SARFA-L300, Mr. John Corrie
1	Library, H1300, Bl. 51-2
	Commander, Harry Diamond Laboratories, 2800 Powder Mill Road, Adelphi, Maryland 20783
1	ATTN: Technical Information Office
	Commander, Picatinny Arsenal, Dover, New Jersey 07801
1	ATTN: SARPA-RT-S
	Commander, Redstone Scientific Information Center, U. S. Army Missile Command, Redstone Arsenal, Alabama 35809
4	ATTN: DRSMI-RBLD, Document Section
	Commander, Watervliet Arsenal, Watervliet, New York 12189
1	ATTN: SARWV-RDT, Technical Information Services Office
	Commander, U. S. Army Foreign Science and Technology Center, 220 7th Street, N. E., Charlottesville, Virginia 22901
1	ATTN: DRXST-SD3
	Director, Eustis Directorate, U. S. Army Air Mobility Research and Development Laboratory, Fort Eustis, Virginia 23604
1	ATTN: Mr. J. Robinson, SAVDL-EU-SS
	Librarian, U. S. Army Aviation School Library, Fort Rucker, Alabama 36360
1	ATTN: Building 5907
	Naval Research Laboratory, Washington, D. C. 20375
1	ATTN: Dr. J. M. Krafft - Code 8430
1	Dr. G. R. Yoder - Code 6382
	Chief of Naval Research, Arlington, Virginia 22217
1	ATTN: Code 471
	Air Force Materials Laboratory, Wright-Patterson Air Force Base, Ohio 45433
2	ATTN: AFML (MXE), E. Morrissey
1	AFML (LC)
1	AFML (LLP), D. M. Forney, Jr.
1	AFML (MBC), S. Schulman
	National Aeronautics and Space Administration, Washington, D. C. 20546
1	ATTN: Mr. B. G. Achhammer
1	Mr. G. C. Deutsch - Code RR-1
	National Aeronautics and Space Administration, Marshall Space Flight Center, Huntsville, Alabama 35812
1	ATTN: R-P&VE-M, R. J. Schwinghamer
1	S&E-ME-MM, Mr. W. A. Wilson, Building 4720

No. of Copies	To
	Wyman-Gordon Company, Worcester, Massachusetts 01601
1	ATTN: Technical Library
	Defense Advanced Research Projects Agency, 1400 Wilson Boulevard, Arlington, Virginia 22209
5	ATTN: Dr. E. C. van Reuth
	National Science Foundation, 1800 G Street, Washington, D. C. 20550
1	ATTN: Dr. Robert Reynik
	General Electric Company, Corporate Research and Development, Schenectady, New York 12301
5	ATTN: Mr. F. X. Gigliotti, Jr.
	Hitchiner Manufacturing Co., Inc., Elm Street, Milford, New Hampshire 03055
5	ATTN: Mr. G. D. Chandley
	Abex Corporation, Research Center, Mahwah, New Jersey 07430
5	ATTN: H. R. Larson
	Massachusetts Institute of Technology, Dept. of Metallurgy and Materials Science, Cambridge, Massachusetts 02139
5	ATTN: Dr. Merton C. Fleming
	TRW Equipment, TRW Inc., 23555 Euclid Avenue, Cleveland, Ohio 44117
1	ATTN: Elizabeth Barrett, T/M 3417
	Deposits & Composites Inc., 1821 Michael Faraday Drive, Reston, Virginia 22090
1	ATTN: Richard E. Engdahl, President
1	Dr. Maurice Sinnott, University of Michigan, Assoc. Dir. of Engineering, Ann Arbor, Michigan 48104
1	Fred E. Ziter, Adirondack Steel Casting Co., Shaker Road, Watervliet, New York 12189
1	Dr. Raymond J. Bratton, Westinghouse Electric Corporation Research Laboratory, Pittsburgh, Pennsylvania 15235
1	W. M. Spurgeon, Director, Mfg., Quality Control & Home Systems, Program Management Center, Bendix Research Laboratories, Bendix Center, Southfield, Michigan 48075
1	S. T. Wlodek, Director of Stellite R&D, Stellite Division, Cabot Corporation, 1020 West Park Avenue, Kokomo, Indiana 46901
1	Mr. William A. Butler, Contract Administrator, Microwave Associates, Inc., Burlington, Massachusetts 01803

No. of Copies	To
1	Mr. John A. Ulrich, Sr. Vice-President, Chamberlain Manufacturing Corp., Waterloo, Iowa 50705
1	A. V. Illyn, Technical Director, Babcock & Wilcox, Old Savannah Road, Augusta, Georgia 30903
1	Mr. W. J. Welsch (Code 224), Naval Materials Industry Resources Office, N.A.E.C., Building #537, Philadelphia, Pennsylvania 19112
1	Mr. R. E. Cross, Federal Die Casting Co., 2222 Elston Avenue, Chicago, Illinois 60614
1	Captain Ebenezer F. Porter, 2618 S. Lynn Street, Arlington, Virginia 22202
1	Mr. Charles E. Bates, Head, Metallurgy Section, Southern Research Institute, 2000 Ninth Avenue, South, Birmingham, Alabama 35205
1	Mr. R. F. Kirby, Chief, Materials Engineering Dept., Dept. 93-39M, Airesearch Manufacturing Company of Arizona, 402 South 36th Street, P. O. Box 5217, Phoenix, Arizona 85010
1	Dr. Mervin T. Rowley, American Foundry Men's Society, Golf & Wolf Roads, Des Plaines, Illinois 60016
1	William R. Freeman, Jr., Howmet Corporation, Vice President and Technical Director, Technical Center, Gas Turbine Components Group, 699 Benston Road, Whitehall, Michigan 49461
1	Dole A. Marek, General Motors Corporation, Detroit Diesel Allison, 4700 W 10th Street, Indianapolis, Indiana 46206
	General Dynamics, Convair Aerospace Division, P. O. Box 748, Ft. Worth, Texas 76101
1	ATTN: Mfg. Engineering Technical Library
1	Dr. Robert Mehrabian, Dept. of Metallurgy & Mining Engineering, University of Illinois, Urbana, Illinois 61801
1	Robert McNally, Research Library, Special Metals Corporation, Middle Settlement Road, New Hartford, New York 13413
	Director, Army Materials and Mechanics Research Center, Watertown, Massachusetts 02172
2	ATTN: DRXMR-PL
1	DRXMR-PR
1	DRXMR-AP
1	DRXMR-CT
1	DRXMR-X
1	DRXMR-D

Army Materials and Mechanics Research Center
Watertown, Massachusetts 02172
NOISE ABATEMENT AND INTERNAL VIBRATIONAL ABSORPTION IN POTENTIAL STRUCTURAL MATERIALS -- L. Kaufman, S. A. Kulin, P. P. Neshe.
Semi-Annual Report AMMRC CTR 76-30, September 1976
80 pp-illus-table, D/A Project ARPA 2555,
AMCMS Code 611102.11.H4200

AD__________ UNCLASSIFIED
UNLIMITED DISTRIBUTION

Key Words
Ships Propellers
Vibration Damping
Cobalt-Iron Alloys
Cobalt-Iron-Manganese Alloys
Iron-Chromium-Aluminum Alloys
Military Reconnaissence Vehicles

Efforts have been directed toward identifying potential structural materials which can combine high strength and damping characteristics in the audible range. Cobalt-iron alloys with additions of aluminum and manganese, copper-aluminum-nickel alloys, iron-chromium-aluminum alloys, titanium-nickel alloys, and several commercial steel compositions have been investigated. The range of yield strengths and loss factors which are attainable exceed currently available commercial materials. A survey of potential applications of high damping alloys to military systems was conducted. Three potential areas which merit consideration include body panels of military reconnaissence vehicles, motor covers and ship propellers. Plans to fabricate body panels for a 1/6 scale dynamic model of an armoured personnel carrier have been made. Measurements of the enthalpy of transformation in a thermoelastic Cu-Al-Ni alloy has been conducted over a range of grain size and sample size to assess the stored elastic strain energy. Studies of the magnetic domain wall configuration in a cobalt-iron alloy have been initialed to evaluate the contribution of domains to damping this alloy.

Army Materials and Mechanics Research Center
Watertown, Massachusetts 02172
NOISE ABATEMENT AND INTERNAL VIBRATIONAL ABSORPTION IN POTENTIAL STRUCTURAL MATERIALS -- L. Kaufman, S. A. Kulin, P. P. Neshe.
Semi-Annual Report AMMRC CTR 76-30, September 1976
80 pp-illus-table, D/A Project ARPA 2555,
AMCMS Code 611102.11.H4200

AD__________ UNCLASSIFIED
UNLIMITED DISTRIBUTION

Key Words
Ships Propellers
Vibration Damping
Cobalt-Iron Alloys
Cobalt-Iron-Manganese Alloys
Iron-Chromium-Aluminum Alloys
Military Reconnaissence Vehicles

Efforts have been directed toward identifying potential structural materials which can combine high strength and damping characteristics in the audible range. Cobalt-iron alloys with additions of aluminum and manganese, copper-aluminum-nickel alloys, iron-chromium-aluminum alloys, titanium-nickel alloys, and several commercial steel compositions have been investigated. The range of yield strengths and loss factors which are attainable exceed currently available commercial materials. A survey of potential applications of high damping alloys to military systems was conducted. Three potential areas which merit consideration include body panels of military reconnaissence vehicles, motor covers and ship propellers. Plans to fabricate body panels for a 1/6 scale dynamic model of an armoured personnel carrier have been made. Measurements of the enthalpy of transformation in a thermoelastic Cu-Al-Ni alloy has been conducted over a range of grain size and sample size to assess the stored elastic strain energy. Studies of the magnetic domain wall configuration in a cobalt-iron alloy have been initialed to evaluate the contribution of domains to damping this alloy.

Army Materials and Mechanics Research Center
Watertown, Massachusetts 02172
NOISE ABATEMENT AND INTERNAL VIBRATIONAL ABSORPTION IN POTENTIAL STRUCTURAL MATERIALS -- L. Kaufman, S. A. Kulin, P. P. Neshe.
Semi-Annual Report AMMRC CTR 76-30, September 1976
80 pp-illus-table, D/A Project ARPA 2555,
AMCMS Code 611102.11.H4200

AD__________ UNCLASSIFIED
UNLIMITED DISTRIBUTION

Key Words
Ships Propellers
Vibration Damping
Cobalt-Iron Alloys
Cobalt-Iron-Manganese Alloys
Iron-Chromium-Aluminum Alloys
Military Reconnaissence Vehicles

Efforts have been directed toward identifying potential structural materials which can combine high strength and damping characteristics in the audible range. Cobalt-iron alloys with additions of aluminum and manganese, copper-aluminum-nickel alloys, iron-chromium-aluminum alloys, titanium-nickel alloys, and several commercial steel compositions have been investigated. The range of yield strengths and loss factors which are attainable exceed currently available commercial materials. A survey of potential applications of high damping alloys to military systems was conducted. Three potential areas which merit consideration include body panels of military reconnaissence vehicles, motor covers and ship propellers. Plans to fabricate body panels for a 1/6 scale dynamic model of an armoured personnel carrier have been made. Measurements of the enthalpy of transformation in a thermoelastic Cu-Al-Ni alloy has been conducted over a range of grain size and sample size to assess the stored elastic strain energy. Studies of the magnetic domain wall configuration in a cobalt-iron alloy have been initialed to evaluate the contribution of domains to damping this alloy.

Army Materials and Mechanics Research Center
Watertown, Massachusetts 02172
NOISE ABATEMENT AND INTERNAL VIBRATIONAL ABSORPTION IN POTENTIAL STRUCTURAL MATERIALS -- L. Kaufman, S. A. Kulin, P. P. Neshe.
Semi-Annual Report AMMRC CTR 76-30, September 1976
80 pp-illus-table, D/A Project ARPA 2555,
AMCMS Code 611102.11.H4200

AD__________ UNCLASSIFIED
UNLIMITED DISTRIBUTION

Key Words
Ships Propellers
Vibration Damping
Cobalt-Iron Alloys
Cobalt-Iron-Manganese Alloys
Iron-Chromium-Aluminum Alloys
Military Reconnaissence Vehicles

Efforts have been directed toward identifying potential structural materials which can combine high strength and damping characteristics in the audible range. Cobalt-iron alloys with additions of aluminum and manganese, copper-aluminum-nickel alloys, iron-chromium-aluminum alloys, titanium-nickel alloys, and several commercial steel compositions have been investigated. The range of yield strengths and loss factors which are attainable exceed currently available commercial materials. A survey of potential applications of high damping alloys to military systems was conducted. Three potential areas which merit consideration include body panels of military reconnaissence vehicles, motor covers and ship propellers. Plans to fabricate body panels for a 1/6 scale dynamic model of an armoured personnel carrier have been made. Measurements of the enthalpy of transformation in a thermoelastic Cu-Al-Ni alloy has been conducted over a range of grain size and sample size to assess the stored elastic strain energy. Studies of the magnetic domain wall configuration in a cobalt-iron alloy have been initialed to evaluate the contribution of domains to damping this alloy.

Army Materials and Mechanics Research Center
Watertown, Massachusetts 02172
NOISE ABATEMENT AND INTERNAL VIBRATIONAL ABSORPTION IN POTENTIAL STRUCTURAL MATERIALS -- L. Kaufman, S. A. Kulin, P. P. Neshe.
Semi-Annual Report AMMRC CTR 76-30, September 1976
80 pp-illus-table, D/A Project ARPA 2555,
AMCMS Code 611102.11.H4200

AD ________ UNCLASSIFIED
UNLIMITED DISTRIBUTION

Key Words
Ships Propellers
Vibration Damping
Cobalt-Iron Alloys
Cobalt-Iron-Manganese Alloys
Iron-Chromium-Aluminum Alloys
Military Reconnaissence Vehicles

Efforts have been directed toward identifying potential structural materials which can combine high strength and damping characteristics in the audible range. Cobalt-iron alloys with additions of aluminum and manganese, copper-aluminum-nickel alloys, iron-chromium-aluminum alloys, titanium-nickel alloys, and several commercial steel compositions have been investigated. The range of yield strengths and loss factors which are attainable exceed currently available commercial materials. A survey of potential applications of high damping alloys to military systems was conducted. Three potential areas which merit consideration include body panels of military reconnaissence vehicles, motor covers and ship propellers. Plans to fabricate body panels for a 1/6 scale dynamic model of an armoured personnel carrier have been made. Measurements of the enthalpy of transformation in a thermoelastic Cu-Al-Ni alloy has been conducted over a range of grain size and sample size to assess the stored elastic strain energy. Studies of the magnetic domain wall configuration in a cobalt-iron alloy have been initialed to evaluate the contribution of domains to damping this alloy.

Army Materials and Mechanics Research Center
Watertown, Massachusetts 02172
NOISE ABATEMENT AND INTERNAL VIBRATIONAL ABSORPTION IN POTENTIAL STRUCTURAL MATERIALS -- L. Kaufman, S. A. Kulin, P. P. Neshe.
Semi-Annual Report AMMRC CTR 76-30, September 1976
80 pp-illus-table, D/A Project ARPA 2555,
AMCMS Code 611102.11.H4200

AD ________ UNCLASSIFIED
UNLIMITED DISTRIBUTION

Key Words
Ships Propellers
Vibration Damping
Cobalt-Iron Alloys
Cobalt-Iron-Manganese Alloys
Iron-Chromium-Aluminum Alloys
Military Reconnaissence Vehicles

Efforts have been directed toward identifying potential structural materials which can combine high strength and damping characteristics in the audible range. Cobalt-iron alloys with additions of aluminum and manganese, copper-aluminum-nickel alloys, iron-chromium-aluminum alloys, titanium-nickel alloys, and several commercial steel compositions have been investigated. The range of yield strengths and loss factors which are attainable exceed currently available commercial materials. A survey of potential applications of high damping alloys to military systems was conducted. Three potential areas which merit consideration include body panels of military reconnaissence vehicles, motor covers and ship propellers. Plans to fabricate body panels for a 1/6 scale dynamic model of an armoured personnel carrier have been made. Measurements of the enthalpy of transformation in a thermoelastic Cu-Al-Ni alloy has been conducted over a range of grain size and sample size to assess the stored elastic strain energy. Studies of the magnetic domain wall configuration in a cobalt-iron alloy have been initialed to evaluate the contribution of domains to damping this alloy.

Army Materials and Mechanics Research Center
Watertown, Massachusetts 02172
NOISE ABATEMENT AND INTERNAL VIBRATIONAL ABSORPTION IN POTENTIAL STRUCTURAL MATERIALS -- L. Kaufman, S. A. Kulin, P. P. Neshe.
Semi-Annual Report AMMRC CTR 76-30, September 1976
80 pp-illus-table, D/A Project ARPA 2555,
AMCMS Code 611102.11.H4200

AD ________ UNCLASSIFIED
UNLIMITED DISTRIBUTION

Key Words
Ships Propellers
Vibration Damping
Cobalt-Iron Alloys
Cobalt-Iron-Manganese Alloys
Iron-Chromium-Aluminum Alloys
Military Reconnaissence Vehicles

Efforts have been directed toward identifying potential structural materials which can combine high strength and damping characteristics in the audible range. Cobalt-iron alloys with additions of aluminum and manganese, copper-aluminum-nickel alloys, iron-chromium-aluminum alloys, titanium-nickel alloys, and several commercial steel compositions have been investigated. The range of yield strengths and loss factors which are attainable exceed currently available commercial materials. A survey of potential applications of high damping alloys to military systems was conducted. Three potential areas which merit consideration include body panels of military reconnaissence vehicles, motor covers and ship propellers. Plans to fabricate body panels for a 1/6 scale dynamic model of an armoured personnel carrier have been made. Measurements of the enthalpy of transformation in a thermoelastic Cu-Al-Ni alloy has been conducted over a range of grain size and sample size to assess the stored elastic strain energy. Studies of the magnetic domain wall configuration in a cobalt-iron alloy have been initialed to evaluate the contribution of domains to damping this alloy.

Army Materials and Mechanics Research Center
Watertown, Massachusetts 02172
NOISE ABATEMENT AND INTERNAL VIBRATIONAL ABSORPTION IN POTENTIAL STRUCTURAL MATERIALS -- L. Kaufman, S. A. Kulin, P. P. Neshe.
Semi-Annual Report AMMRC CTR 76-30, September 1976
80 pp-illus-table, D/A Project ARPA 2555,
AMCMS Code 611102.11.H4200

AD ________ UNCLASSIFIED
UNLIMITED DISTRIBUTION

Key Words
Ships Propellers
Vibration Damping
Cobalt-Iron Alloys
Cobalt-Iron-Manganese Alloys
Iron-Chromium-Aluminum Alloys
Military Reconnaissence Vehicles

Efforts have been directed toward identifying potential structural materials which can combine high strength and damping characteristics in the audible range. Cobalt-iron alloys with additions of aluminum and manganese, copper-aluminum-nickel alloys, iron-chromium-aluminum alloys, titanium-nickel alloys, and several commercial steel compositions have been investigated. The range of yield strengths and loss factors which are attainable exceed currently available commercial materials. A survey of potential applications of high damping alloys to military systems was conducted. Three potential areas which merit consideration include body panels of military reconnaissence vehicles, motor covers and ship propellers. Plans to fabricate body panels for a 1/6 scale dynamic model of an armoured personnel carrier have been made. Measurements of the enthalpy of transformation in a thermoelastic Cu-Al-Ni alloy has been conducted over a range of grain size and sample size to assess the stored elastic strain energy. Studies of the magnetic domain wall configuration in a cobalt-iron alloy have been initialed to evaluate the contribution of domains to damping this alloy.